Injector Beam Studies April 25-26, 2003

B. Humensky, L. Kaufman, and K. Paschke

Internal HAPPEX Tech Note

June 5, 2003

Contents

1 Introduction

This tech note describes results from the Injector Beam Studies conducted April 25-26, 2003.

2 Calibrating BCMs and BPMs

In order to achieve the necessary precision for measurements of helicity-correlated (HC) charge asymmetry and position differences, it is necessary to determine pedestals for BCM and BPM readouts which account for the nonlinearity of the signal at low currents. This

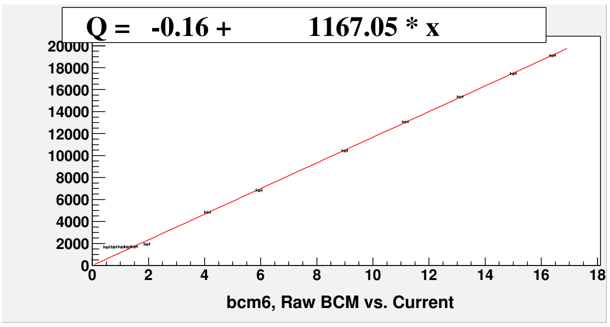

Figure 1: BCM 0L02 vs. Beam current measured in Faraday cup 2. Fit is for $I > 4\mu$A. (Pedestal has already been corrected for this data. Vertical axis is in units of ADC channels.)

low-current non-linearity creates an effective pedestal offset, which can dilute or distort a precision measurement.

The first step in the April beam studies was a calibration of pedestals for all monitors in the data stream. This is done as a "current calibration", with data taken at several beam currents. The current for each data point is measured using the EPICs readout of Faraday Cup #2, which is both very linear and low-pedestal. This Faraday cup is the standard "golden" measurement of current used by MCC.

The EPICs readout of BCM 0L02 showed some non-linearity or gain mis-calibration over current range (0.25-16 μA), reading slightly higher than FC2 above 5μA and slightly lower below. This is important to note because MCC believes that this monitor was properly calibrated, and the deviation from EPICS readbacks of BCM 0L02 and FC2 demonstrate the precision with which one might expect MCC to quote a current setting.

Fig. 1 shows the determination of the effective pedestal for BCM 0L02. The intercept of a linear fit to data points $> 4\mu$A verifies the calibrated pedestal used for this plot. The deviation from linear of the electronics pedestal (near 1800 ADC channels over the calibrated pedestal) is clearly seen.

Fig. 2 shows similar residual fits for BPMs in the 100 keV and 5 MeV regions which were readout using a V2F and scaler. Again, linear fits using only data $> 4\mu$A were performed. These plots are not pedestal subtracted. The deviation between the data at low currents and the extrapolated intercept of the fits demonstrates the need for careful pedestal calibration. Residuals for these fits are shown in Fig. 3. For data $> 4\mu$A, residuals are typically < 200 counts in magnitude, while raw signals are typically $> 20,000$ counts, leading to an estimate of 1% non-linearity for individual BPM wires.

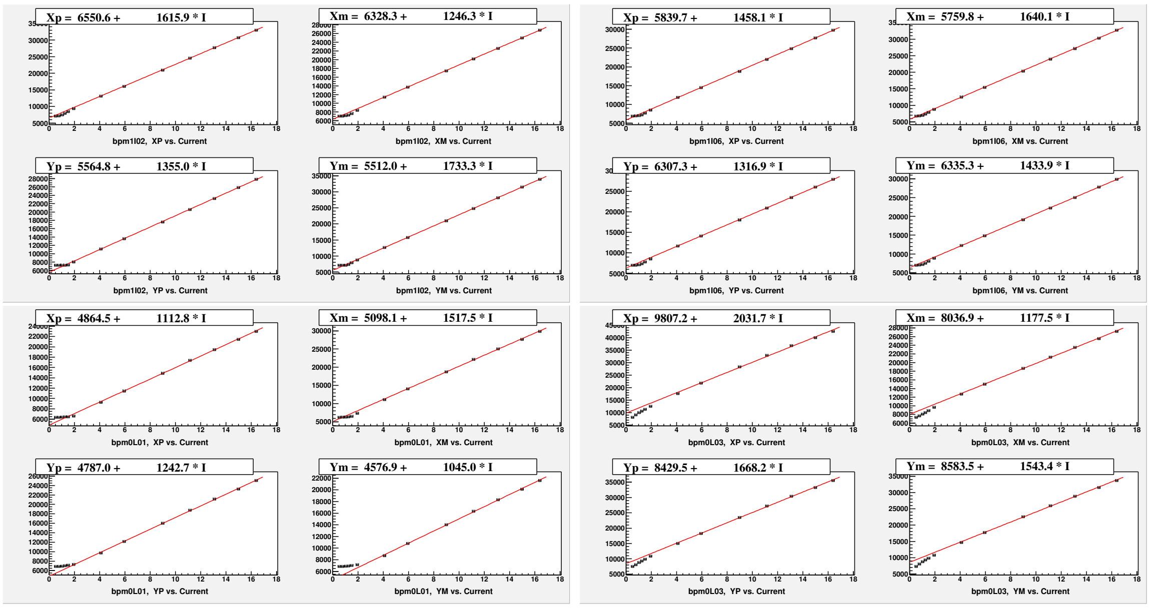

Figure 2: BPM wire readbacks vs. beam current measured in Faraday Cup 2. Fit is for $I > 4\mu$A. Figures include only BPMs readout using V2F. (Vertical axis is in units of scaler counts.)

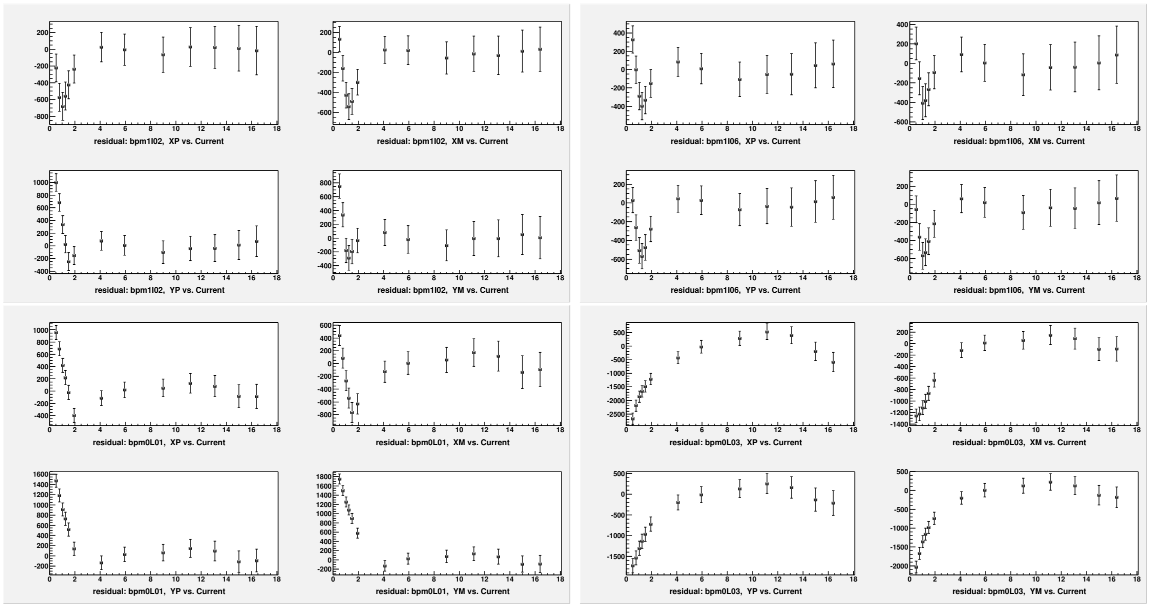

Figure 3: Residuals for fit of BPM wire readbacks vs. beam current. Figures include only BPMs readout using V2F. (Vertical axis is in units of scaler counts.)

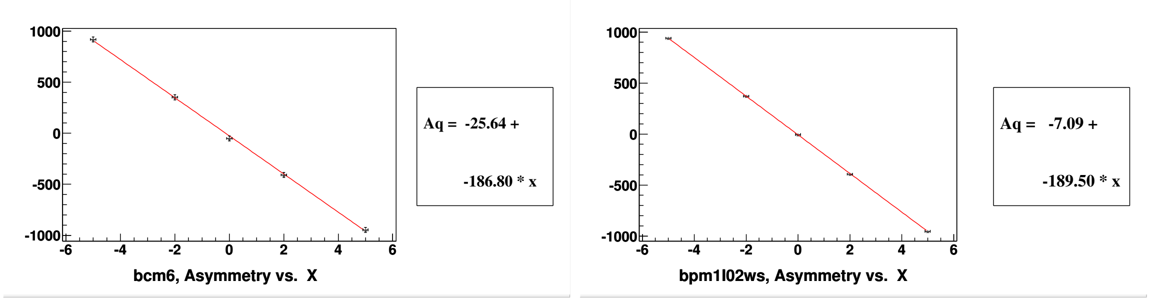

Figure 4: IA calibration scans: Charge asymmetry (in ppm) measured by BCM 0L02 and BPM 1I02 vs. IA setpoint. This is with the original position of the IA waveplate.

3 IA Cell Calibration

The sensitivity of the IA system is determined by the retardation and orientation of a waveplate between aligned linear polarizers. In the present configuration, a halfwave plate is used to create the offset from perfect transmission. The orientation of this waveplate is controlled remotely by a picomotor ("Picomotor S2"). Prior experience has taught us that the picomotor movement and position encoder is very unreliable, so that positions are not repeatable. Any changes to the orientation produce unreliable, and unrepeatable, results, so the process of configuring the waveplate orientation to produce the desired sensitivity is purely empirical.

An original calibration run was taken, finding a slope of 180 ppm/V. This slope would be large enough for HAPPEX, as we plan to keep the charge asymmetry low by tuning the PITA voltages and using the IA cell for corrections of less than 100 ppm. A larger slope was desired in order to make feedback for GDH more reliable (less likely to rail at maximum or minimum setpoint).

The charge asymmetry at the IA zero setpoint was measured, and the IA was then set to its maximum setpoint. Changes in the charge asymmetry could be compared to the original measurement of IA=0 to determine an approximate slope. One step (of 1000 units on the picomotor encoder) was made, and the slope was seen to change to $\sim$ 400ppm/V. The corresponding dynamic range is approximately $\pm$2000 ppm, which is considered to be large enough for a robust feedback system for GDH. An IA calibration scan was taken for the new configuration, to provide a measurement for use by feedback during GDH.

Plots from the first and second calibration runs are shown in Figures 4 and 5. These figures show charge asymmetry at both BCM 0L02 (downstream of the A1 and A2 apertures and the Master Slit) and BPM 1I02, which is the most upstream of the BPMs, closest to the cathode, with no known apertures between the cathode and the BPM. As expected, there is very good agreement in A_Q effect of the IA between the 1I and 0L regions.

3.1 Correlation of Position Differences with IA Voltage

The position differences (in μm) measured at the 100 keV BPMs for the calibration scans are shown in Figures 6 and 7. The position difference behavior is not easily summarized, although for most BPMs, the position sensitivity appears to drop after the waveplate was rotated to increase the IA effect. Before the waveplate rotation, the position sensitivity is as large as 0.5 nm/ppm of A_Q change for some BPMs. If HAPPEX-II uses the IA cell

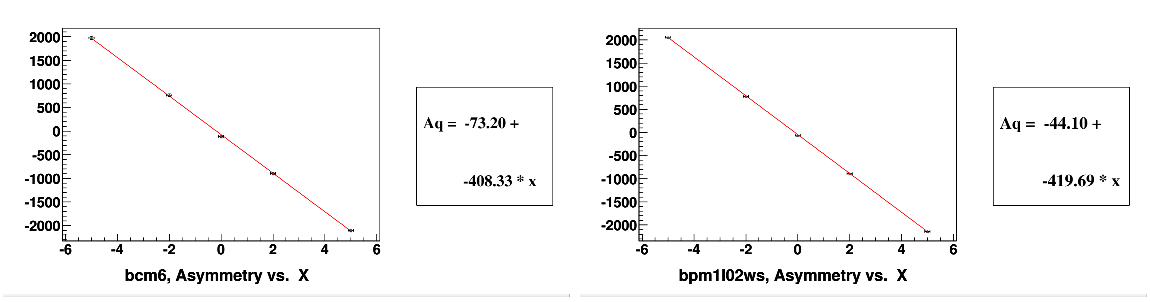

Figure 5: IA calibration scans: Charge asymmetry (in ppm) measured by BCM 0L02 and BPM 1I02 vs. IA setpoint. The position of the IA waveplate has been adjusted to increase the IA lever arm.

to correct $A_Q < 200$ ppm (as expected), then this implies an acceptable position effect of < 100 nm.

Similar plots for the the 5 MeV BPMs are shown in Figures 8 and 9.

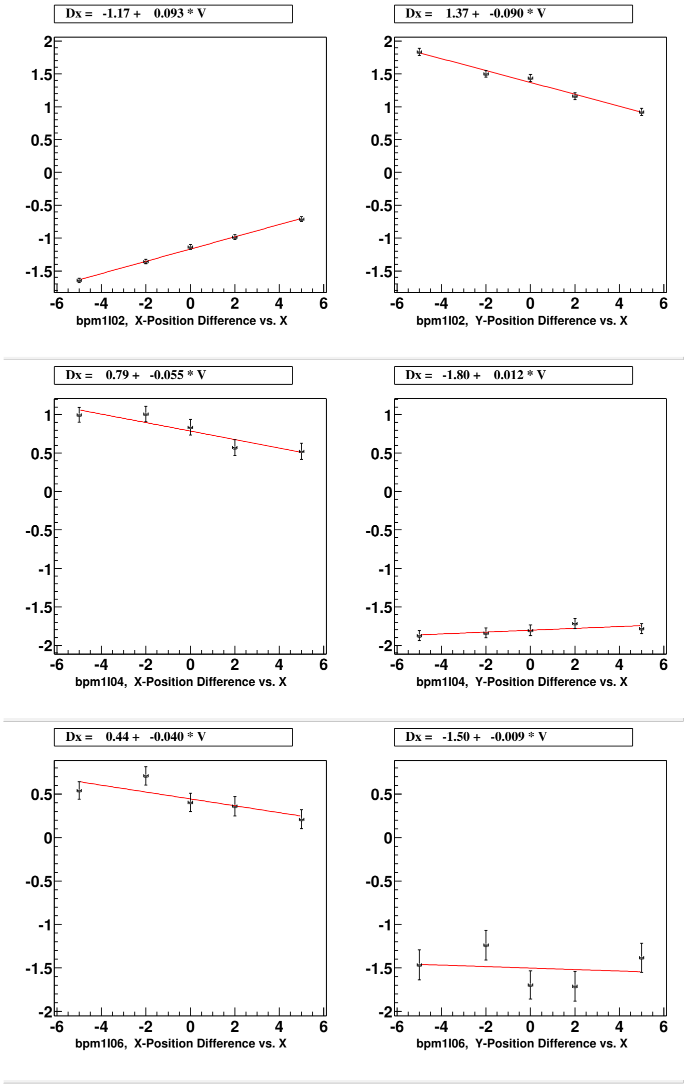

Figure 6: IA calibration scans: Position differences (in μm) measured by 100 keV BPMs vs. IA setpoint. This is with the original position of the IA waveplate ($\mathrm{d}A_Q/\mathrm{dV} \sim 190\mathrm{ppm/V}$).

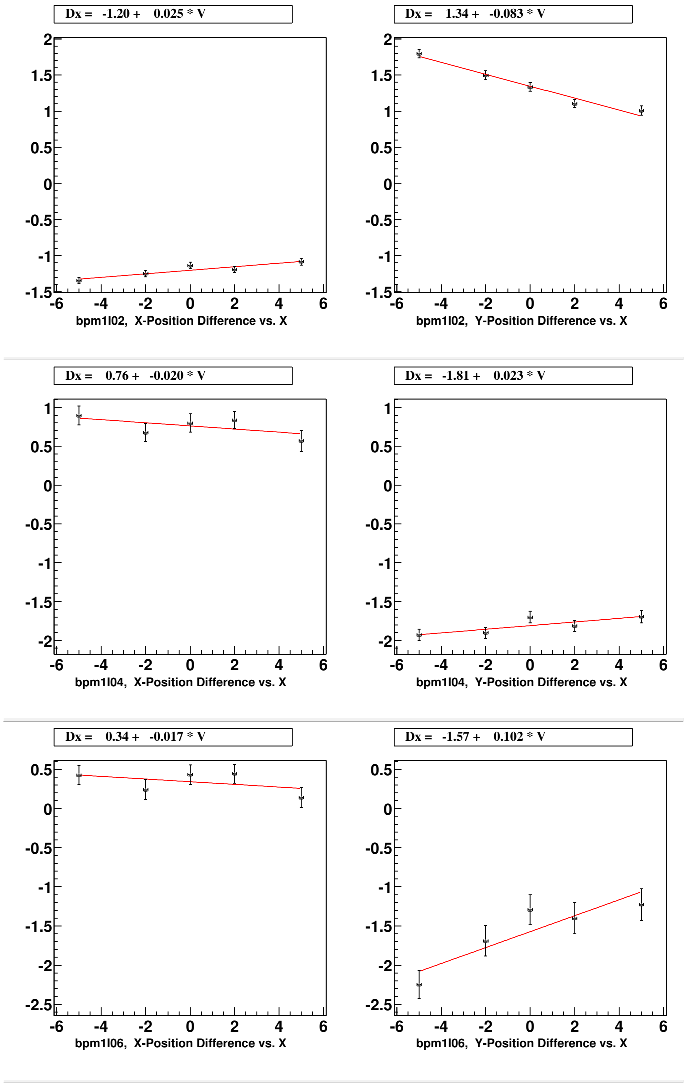

Figure 7: IA calibration scans: Position differences (in μm) measured by 100 keV BPMs vs. IA setpoint. The position of the IA waveplate has been adjusted to increase the IA lever arm ($\mathrm{d}A_Q/\mathrm{dV} \sim 410\mathrm{ppm/V}$).

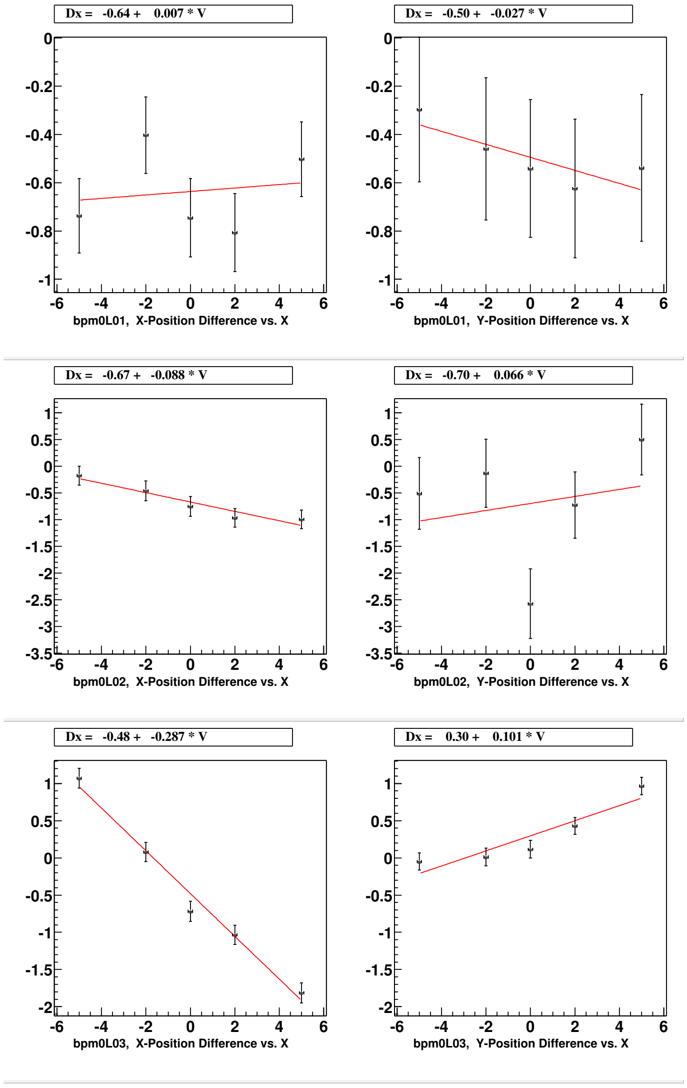

Figure 8: IA calibration scans: Position differences (in μm) measured by 5 MeV BPMs vs. IA setpoint. This is with the original position of the IA waveplate ($dA_Q/dV \sim 190$ppm/V).

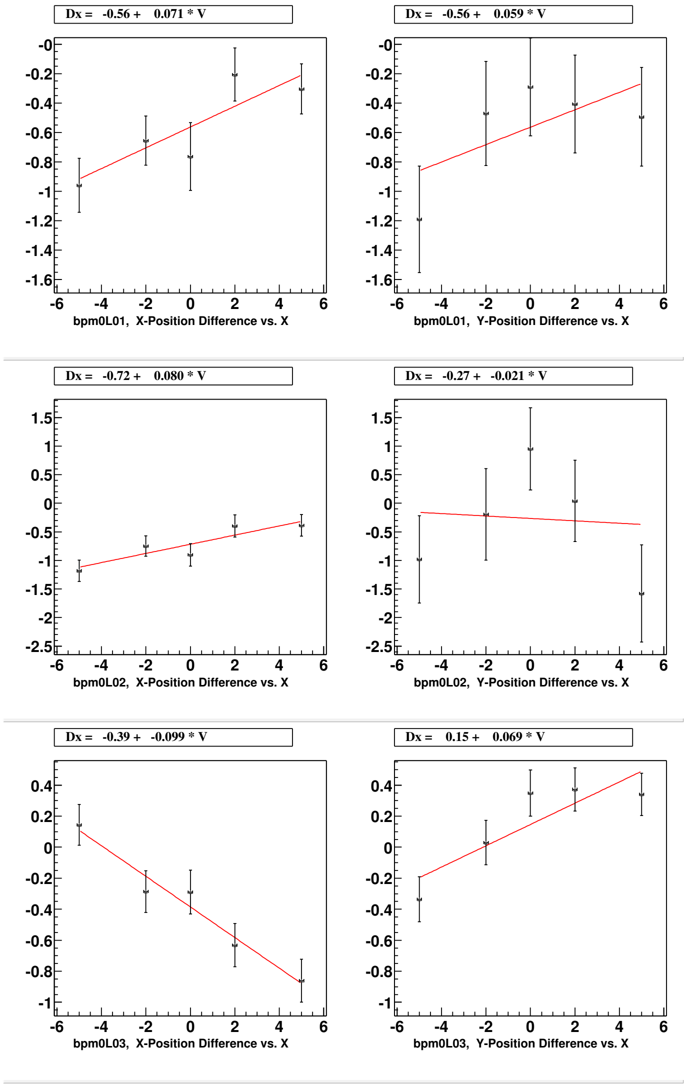

Figure 9: IA calibration scans: Position differences (in μm) measured by 5 MeV BPMs vs. IA setpoint. The position of the IA waveplate has been adjusted to increase the IA lever arm ($\mathrm{d}A_Q/\mathrm{dV} \sim 190\mathrm{ppm/V}$).

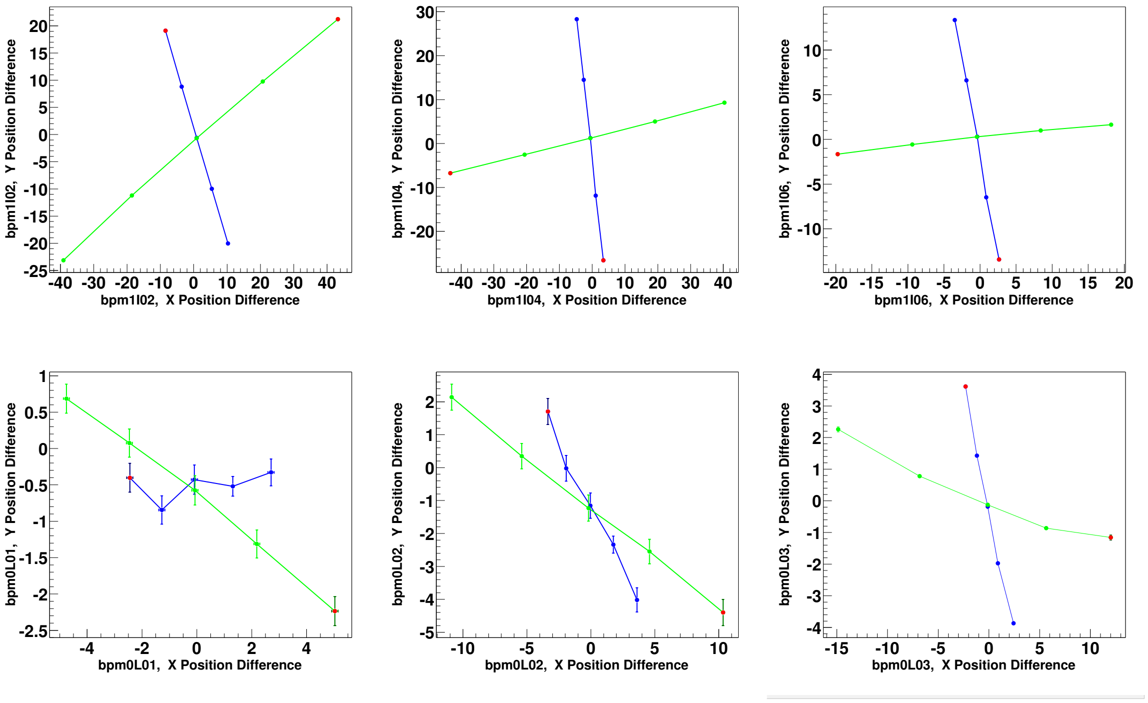

Figure 10: Helicity-correlated position differences for PZT X and Y scans (difference orbit measurements) at 100 keV and 5 MeV BPMs. PZT X scan shown in green, PZT Y scan in blue. One extreme for each scan is marked in red, to show sign-flip of response.

4 PZT Mirror Scans

A mirror in the Hall A laser optics line (before beams for all Halls are combined) is mounted on a piezo-electric-actuated mount. This mirror is used to produce helicity-correlated deflection of the laser spot.

4.1 Propagation of Position Differences through Injector

The changes in mirror-induced position differences as the beam propagates through the injector, shown in Fig 10, provide information on beam transport. The motion of the laser spot induced by PZT X and Y deflection may not be orthogonal, due to imperfections in the mirror mechanism. However, the evolution of the angle between the difference-orbit-changes for the X and Y mirror scans provides information on the orthogonality of beam transport. The size and direction of the difference-orbit changes over the PZT scans provide empirical information on the size of the accelerator beta function at each BPM.

4.2 Correlation of Charge Asymmetry with PZT Voltage

There is a significant correlation between charge asymmetry and PZT setpoint in measured at the first BPM in the 100 keV region, BPM 1I02, as shown in Fig. 11. This is before any beam defining apertures, so such a response is not expected.

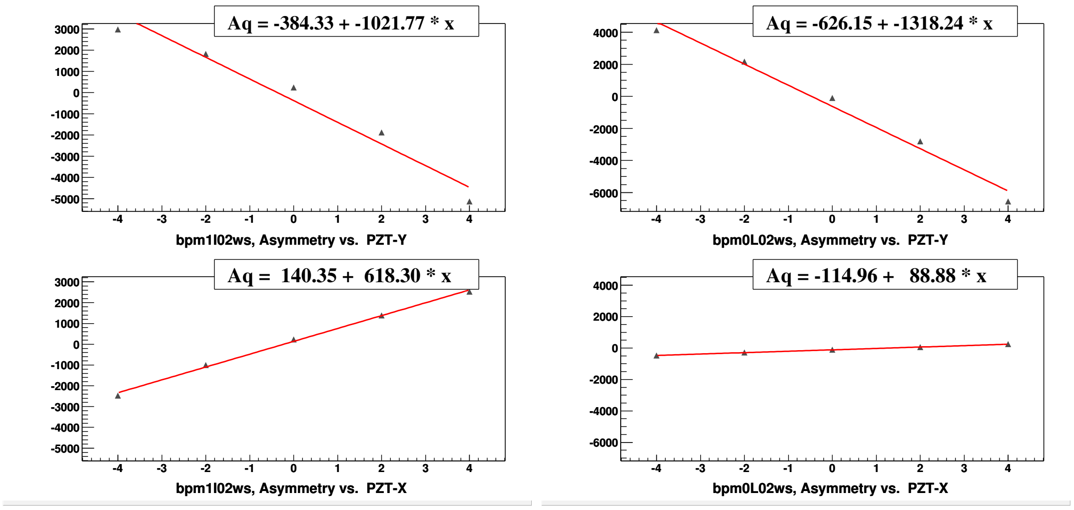

Figure 11: Helicity-correlated charge asymmetry for PZT X and Y scans (difference orbit measurements) at 100 keV (left) and 5 MeV (right) BPMs. PZT Y scans shown above, PZT X scans below.

One possible cause of the charge response would be clipping of the laser beam by optics between the mirror and the cathode, or position-dependent clipping of the electron beam from the cathode. Another possible cause of such a response is a gradient in the the quantum efficiency (QE) of the photocathode. The full range of the spot motion on the photocathode surface is estimated to be around 30 μm, while the beam spot is around 500 μm. The movement is approximately 6% of the beam spot diameter, and the corresponding change in asymmetry $A_Q = \frac{\Delta Q}{2Q}$ is approximately 1%, so the QE gradient across the beam spot necessary to create such an intensity change of this slice of the beam spot is $2 \times 1\%/6\% \approx 33\%$ relative QE change over 500 μm.

In BPM 0L02, the charge response of the X and Y PZT scans have changed significantly. The difference between the 100 keV and 5MeV regions are due to the beam clipping through apertures or on the Master Slit between those sets of BPMs.

5 Source Configuration Procedure

It is necessary to choose rotating halfwave plate (RHWP) orientations for both insertable halfwaveplate (IHWP) states that will meet several criteria:

- small (few hundred ppm) charge asymmetry for each IHWP state.
- small but not negligible PITA slope, ideally near 5-10 ppm/Volt. The PITA slope must be large enough so that the charge asymmetry can be zeroed with a reasonable voltage offset ($<$ 200 Volts), but a large PITA slope increases history-dependent multi-peaking and probably increases higher-order HC systematics (such as spot size asymmetry).
- Small average position differences after IHWP cancellation.
- Small position differences in each IHWP state, to reduce non-linear effects.

When choosing a RHWP angle using these criteria, it is common to choose reasonable RWP setpoints and then use the PITA voltage to reduce the charge asymmetry for each IHWP state. However, there are mechanisms (specifically, gradients of analyzing power of the photocathode) which can create position difference sensitivity to PITA voltage. There are also measurement systematics (specifically, pedestal error) which can couple charge asymmetry to position difference measurement. In order to eliminate a possible influence from either of these effects, it was decided to base the decision on RHWP orientation on scans done which zeroed charge asymmetry at each point using PITA voltage.

Previous investigations have revealed a significant time-drift in retardation over the 30 ms helicity window at the halfwave-voltage setpoints, as well as significant memory effects, which leads to a large differences in average retardation for helicity windows depending on the history of preceding helicity states. The largest effect is seen as a difference between Right-Left pairs preceded by a Right window and Left-Right pairs preceded by a Left helicity window. The difference in charge asymmetry for these two "asymmetric history" combinations (R-RL and L-LR) has been found to have a constant proportionality to PITA slope for all waveplate angles. Thus, the "problem" of the 4-peaks in charge asymmetry which has been recently studied becomes a useful diagnostic of source behavior: knowledge of the PITA slope at one RWP setpoint, and the charge separation as a function of RHWP setting, provides a method for prediction of PITA slope at all RHWP setpoints.

In summary, the source configuration procedure was as follows:

- A PITA scan was taken at the initial RHWP setpoint, to estimate the proportionality constant between PITA slope and "asymmetric-pair" A_Q peak separation.
- RWP scans were performed for each IHWP state.
- With this result, the "peak separation" for each initial RHWP scan was used to derive the PITA slope for each RHWP orientation. This, along with the charge asymmetry for each RHWP orientation, was used to generate a table of PITA voltage offsets to be applied in a second RHWP scan.
- A second scan was performed for each IHWP state, now using those results to zero charge asymmetry at each angle.

5.1 RHWP Scans: Charge Asymmetry

The charge asymmetry from waveplate scans performed for both IHWP states can be seen in Fig. 12 and Fig. 13. Due to an error in conducting the test plan, the Pockels cell voltages were slightly offset (corresponding to a PITA offset of 28 Volts) for the IHWP=OUT run (Fig. 12). This mistake would change the amplitudes, but not the phases, of the terms in the function describing the charge asymmetry response to the RHWP. The charge-asymmetry separation for symmetric pairs and asymmetric pairs for these runs can be seen in Fig. 14 and Fig. 15. The asymmetric-pair charge-asymmetry separation was used to estimate the PITA slope for each RHWP angle, and the Pockels cell voltages were adjusted to zero charge asymmetry during a second set of RHWP scans. The PITA offset applied at each RHWP angle is plotted in Fig. 16 and Fig. 17. The (reduced) charge asymmetry and (unchanged) peak separation for one of those ("RHWP+PITA") scans can be seen in Fig. 18 and Fig. 19. The shape of the charge asymmetry plot (Fig. 18) is unpredictable, and can be large, near nodes in the PITA slope curve.

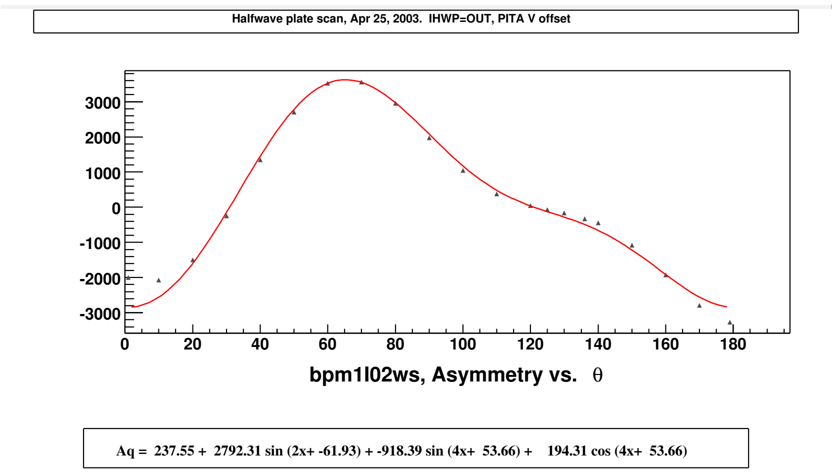

Figure 12: Charge asymmetry (in ppm) measured in BPM 1I02 during rotating waveplate scan. Insertable Halfwave Plate (IHWP) is OUT. PITA voltage is slightly offset (P+= 7.154,P-= 7.527).

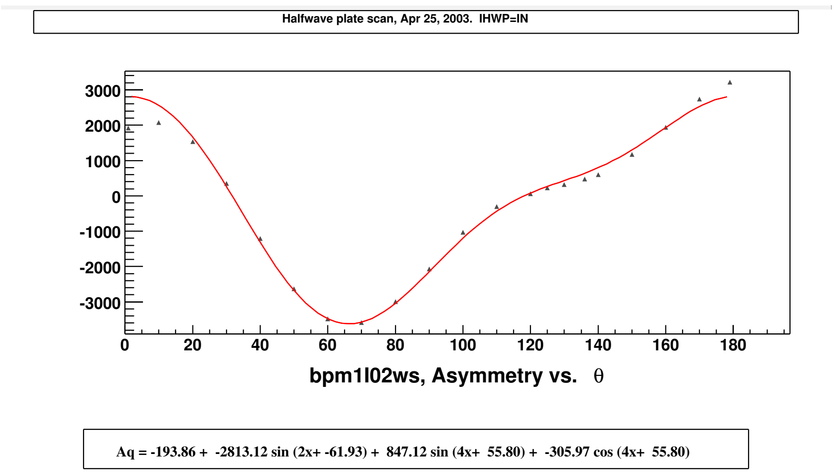

Figure 13: Charge asymmetry (in ppm) measured in BPM 1I02 during rotating waveplate scan. Insertable Halfwave Plate (IHWP) is IN. (PITA voltage P+= 7.224, P-= 7.457)

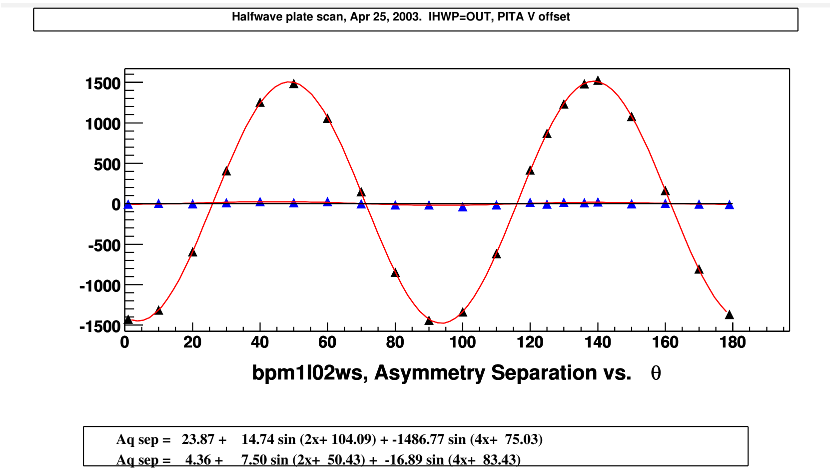

Figure 14: Separation between inner and outer peaks of charge asymmetry (in ppm) measured in BPM 1I02 during rotating waveplate scan. IHWP is OUT. PITA voltage is slightly offset (P+= 7.154,P-= 7.527).

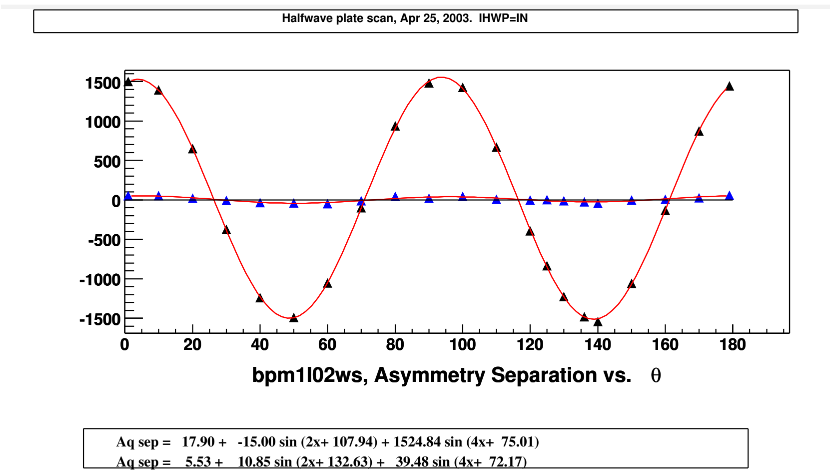

Figure 15: Separation between inner and outer peaks of charge asymmetry (in ppm) measured in BPM 1I02 during rotating waveplate scan. IHWP is IN. (PITA voltage P+= 7.224, P-= 7.457)

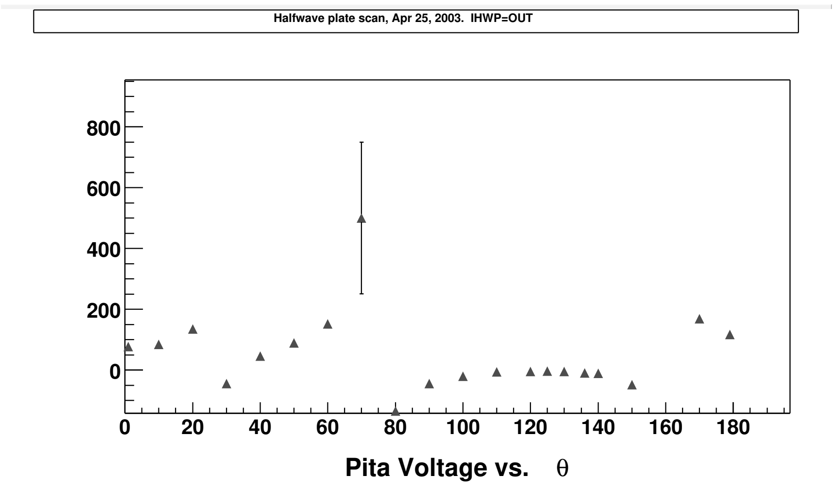

Figure 16: PITA voltage offset applied as a function of waveplate angle for PITA-optimized RHWP scans. Error bars indicate statistical uncertainty in calculation of optimum voltage. If PITA offset magnitude larger than 500 V was indicated, the magnitude was reduced to 500 V (and a large uncertainty displayed). There results apply to IHWP=OUT.

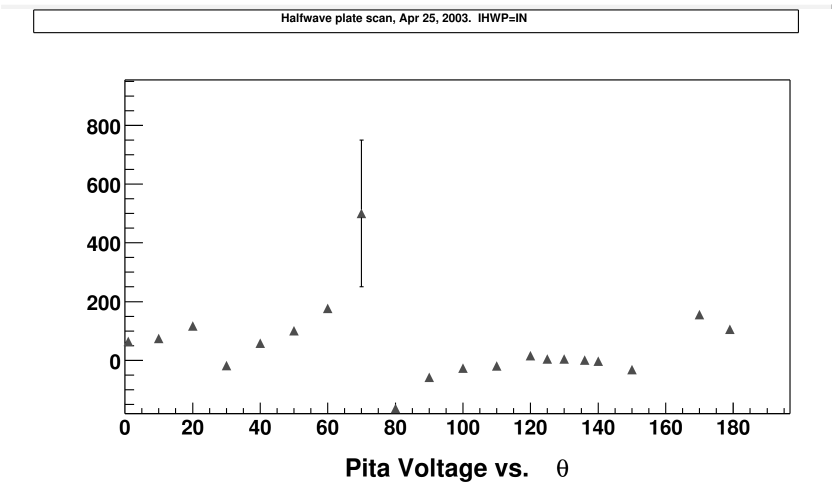

Figure 17: PITA voltage offset applied as a function of waveplate angle for PITA-optimized RHWP scans. Error bars indicate statistical uncertainty in calculation of optimum voltage. If PITA offset magnitude larger than 500 V was indicated, the magnitude was reduced to 500 V (and a large uncertainty displayed). There results apply to IHWP=IN.

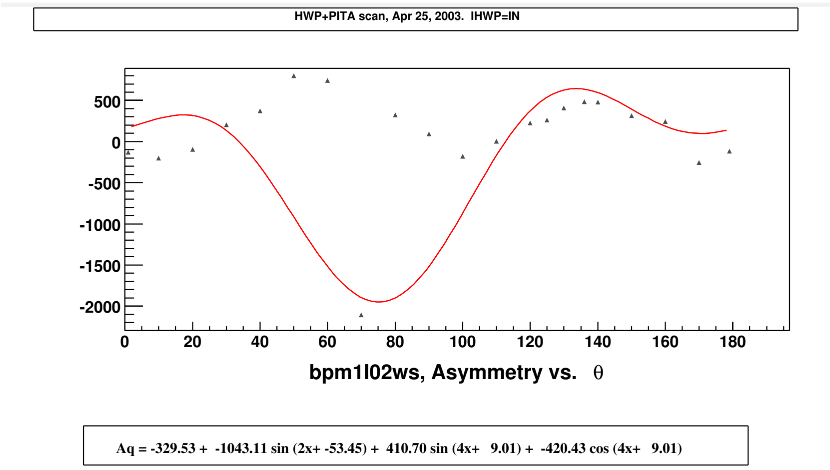

Figure 18: Charge asymmetry (in ppm) measured in BPM 1I02 during rotating waveplate scan, with the PITA voltage at each waveplate setting used to zero charge asymmetry. Insertable Halfwave Plate (IHWP) is IN. The displayed fit function is not expected to represent this data.

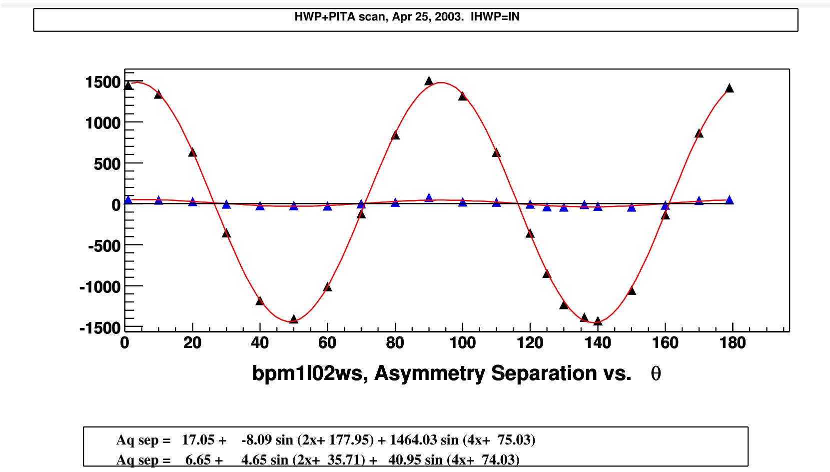

Figure 19: Separation between inner and outer peaks of charge asymmetry (in ppm) measured in BPM 1I02 during rotating waveplate scan, with the PITA voltage at each waveplate setting used to zero charge asymmetry. Insertable Halfwave Plate (IHWP) is IN. Compare to Fig.15.

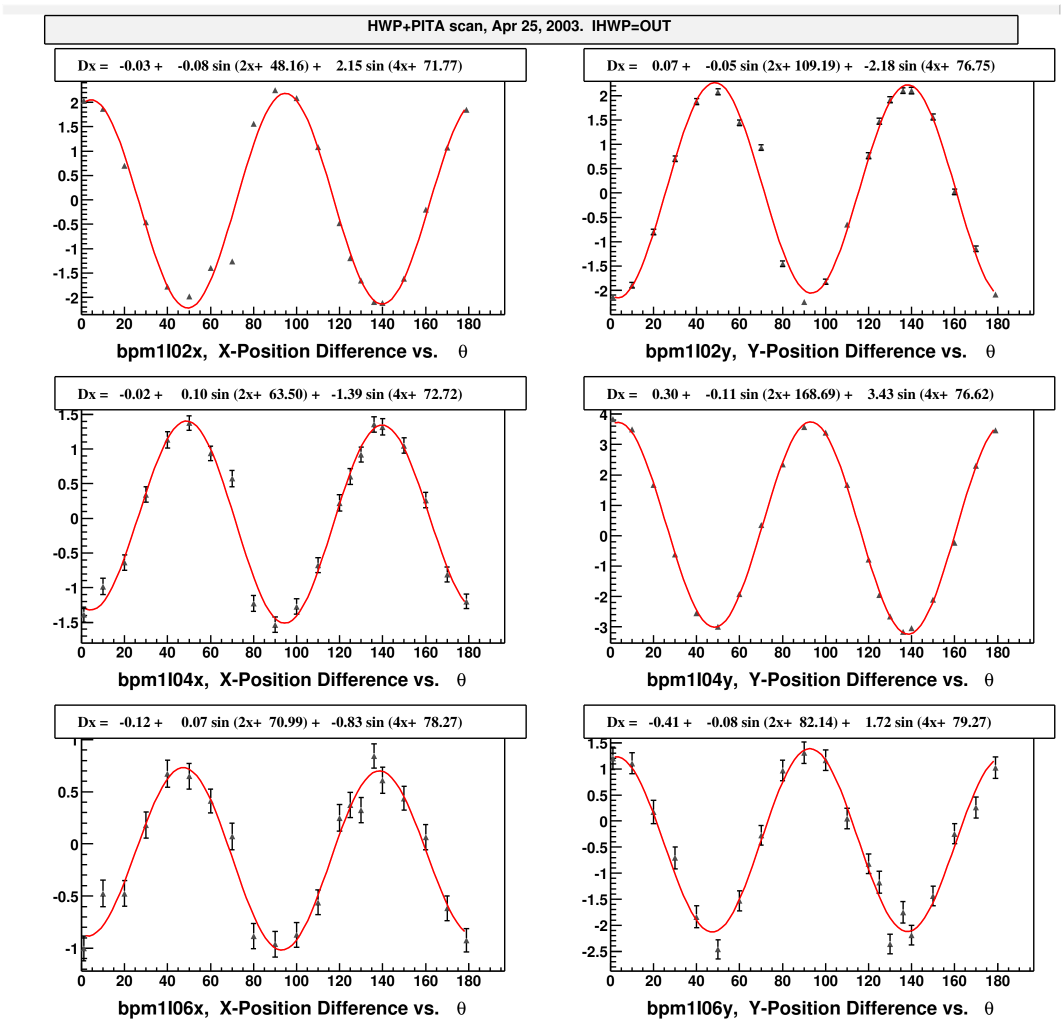

Figure 20: Position differences (in μm) measured by 100 keV BPMs during rotating waveplate scan, with the PITA voltage at each waveplate setting used to zero charge asymmetry. Insertable Halfwave Plate (IHWP) is OUT. Compare to Fig. 24.

5.2 RHWP Scans: Position Differences

The position differences for the "RHWP+PITA" scans were used to select an appropriate angle for the RWP. These position differences in the 100 keV region for both states of the IHWP are shown in Fig. 20 and Fig. 21. The position differences for these runs measured in the 5 MeV region are shown in Fig. 22 and Fig. 23.

Although they were not considered in the process of selecting an RHWP setpoint, the position difference for RHWP scans with constant PITA offsets show a much cleaner fit to the standard $(4\theta + 2\theta)$ function than do the RHWP+PITA scans. This can be seen in Figs. 24 & 25 for 100 keV, and Figs. 26 & 27 for 5 MeV BPMs.

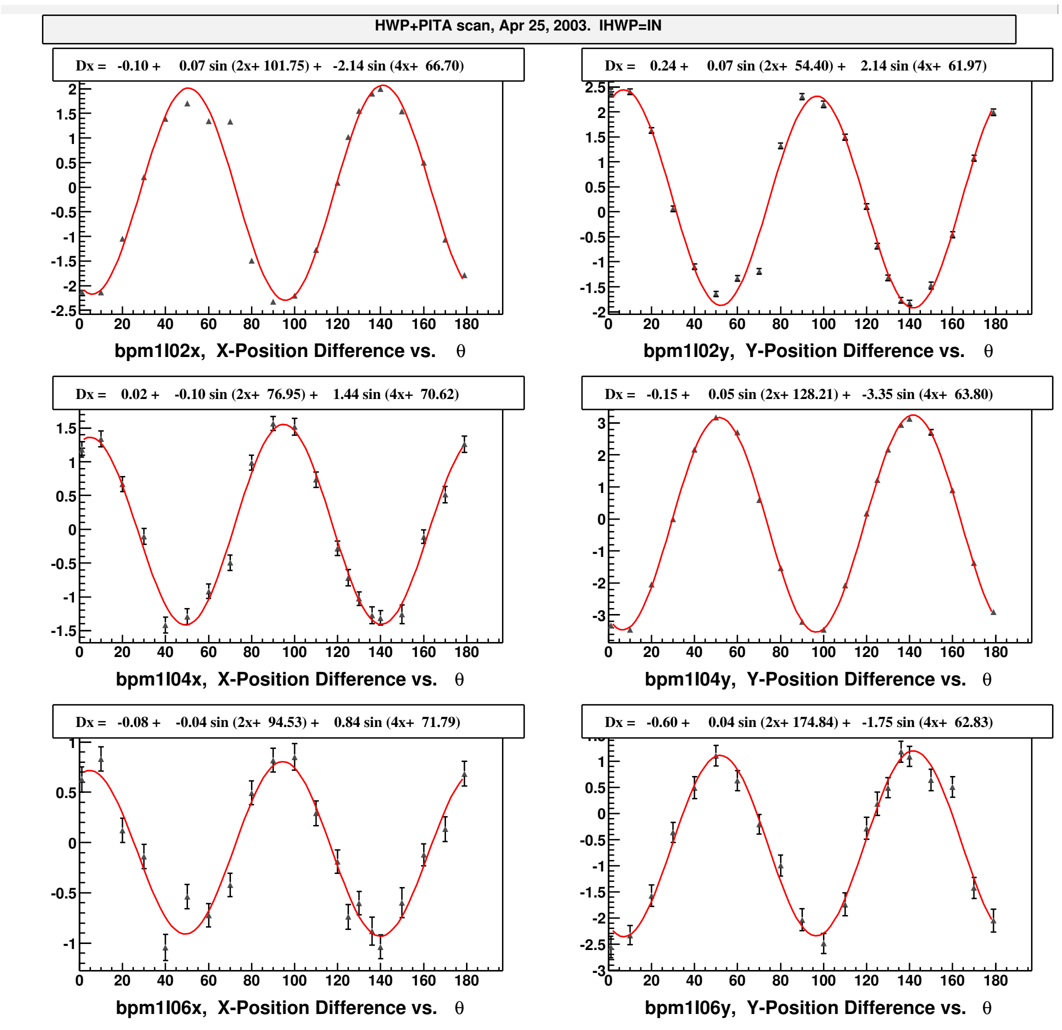

Figure 21: Position differences (in μm) measured by 100 keV BPMs during rotating waveplate scan, with the PITA voltage at each waveplate setting used to zero charge asymmetry. Insertable Halfwave Plate (IHWP) is IN. Compare to Fig. 25.

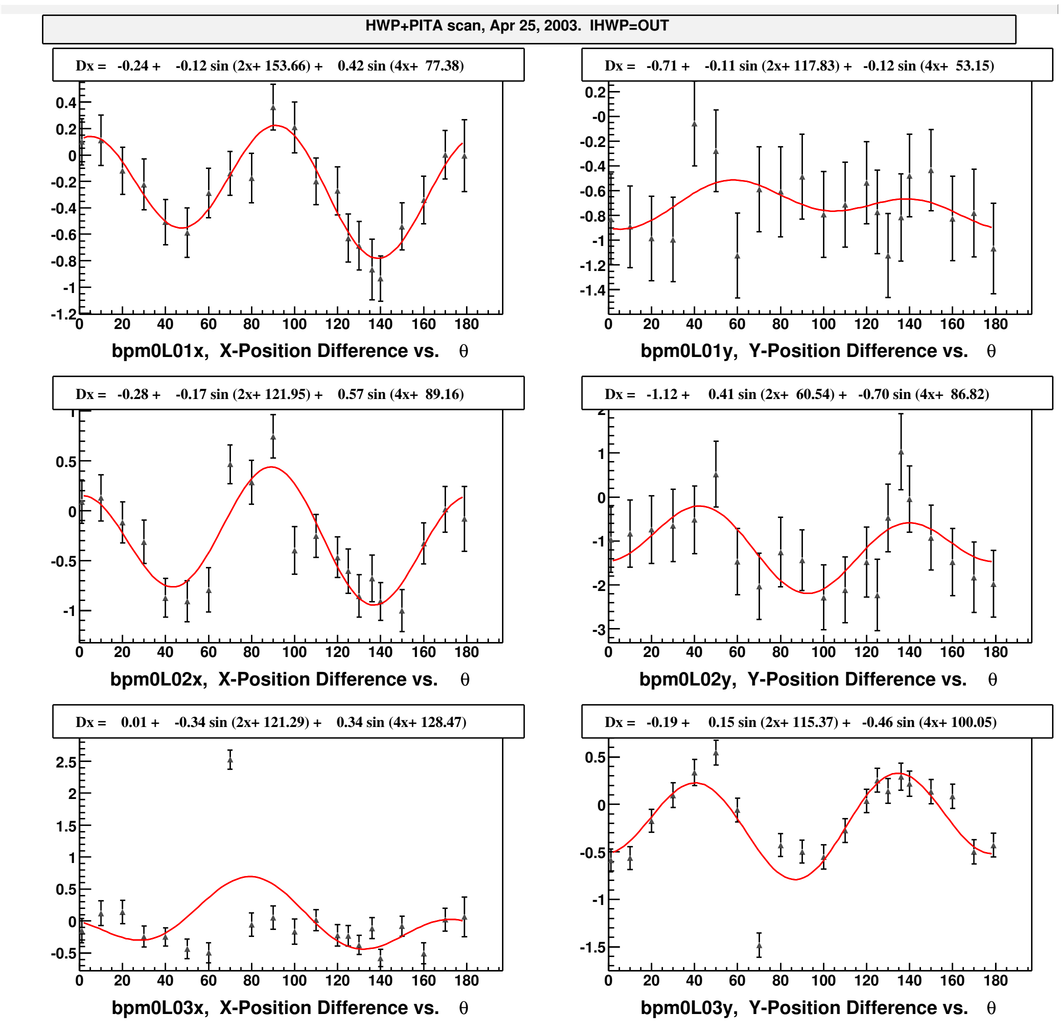

Figure 22: Position differences (in μm) measured in 5 MeV BPMs during rotating waveplate scan, with the PITA voltage at each waveplate setting used to zero charge asymmetry. Insertable Halfwave Plate (IHWP) is OUT. Compare to Fig. 26.

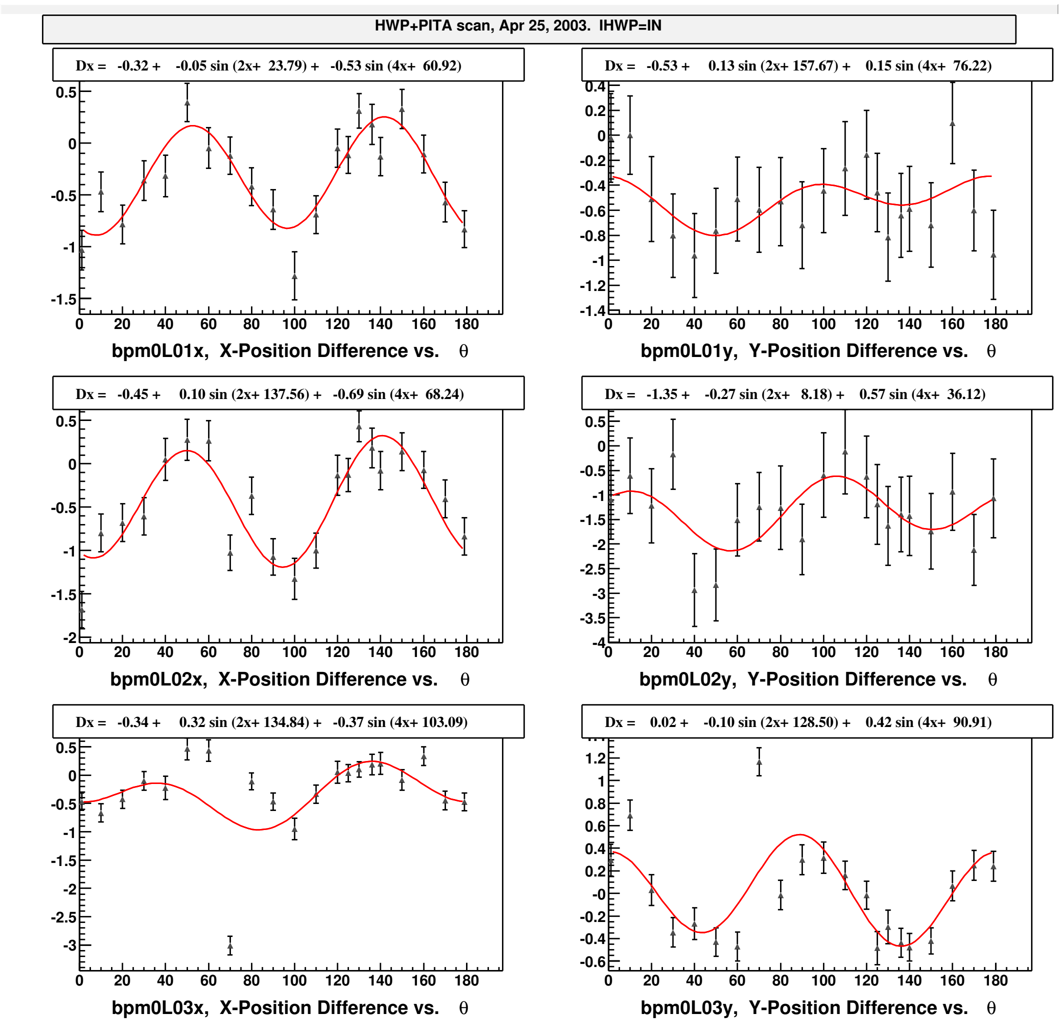

Figure 23: Position differences (in μm) measured in 5 MeV BPMs during rotating waveplate scan, with the PITA voltage at each waveplate setting used to zero charge asymmetry. Insertable Halfwave Plate (IHWP) is IN. Compare to Fig. 27.

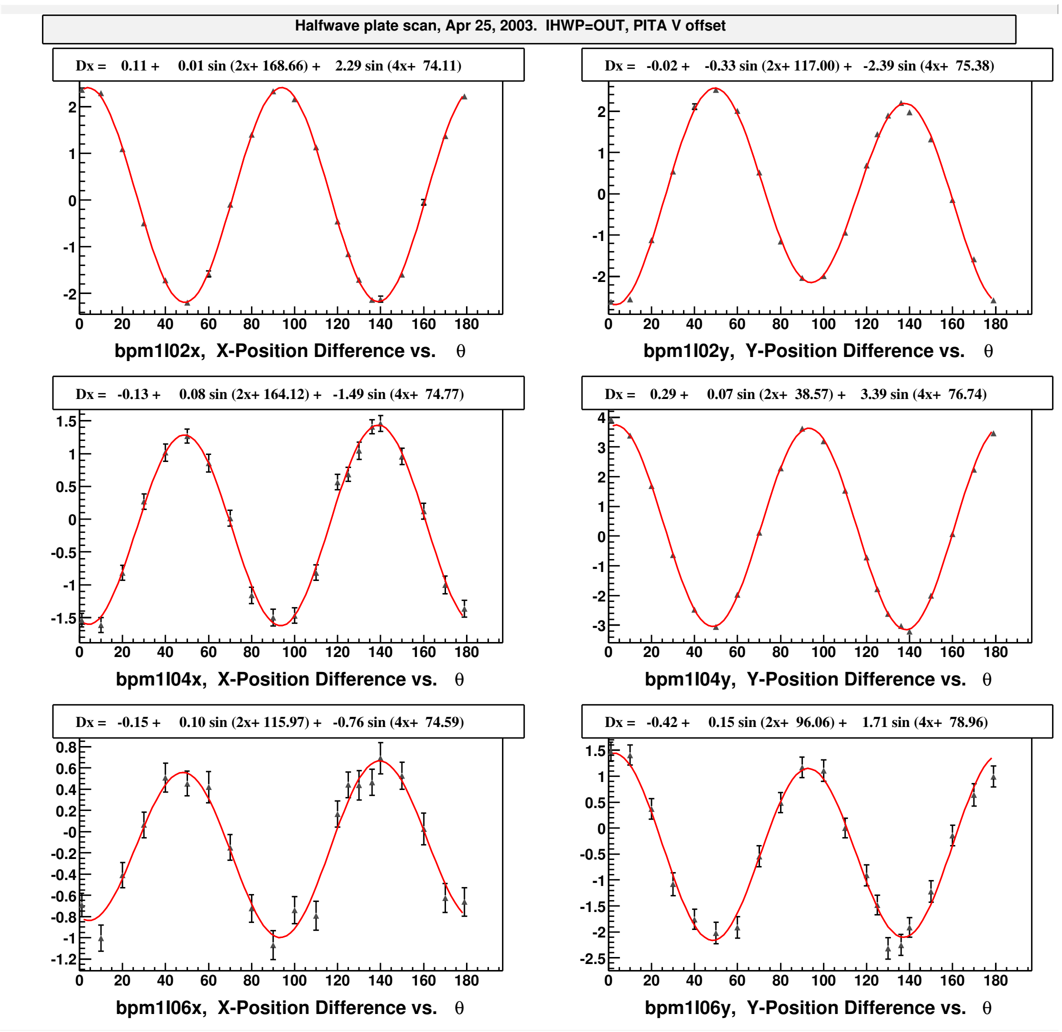

Figure 24: Position differences (in μm) measured by 100 keV BPMs during rotating wave-plate scan. Insertable Halfwave Plate (IHWP) is OUT. PITA voltage is slightly offset (P+=7.154,P-=7.527).

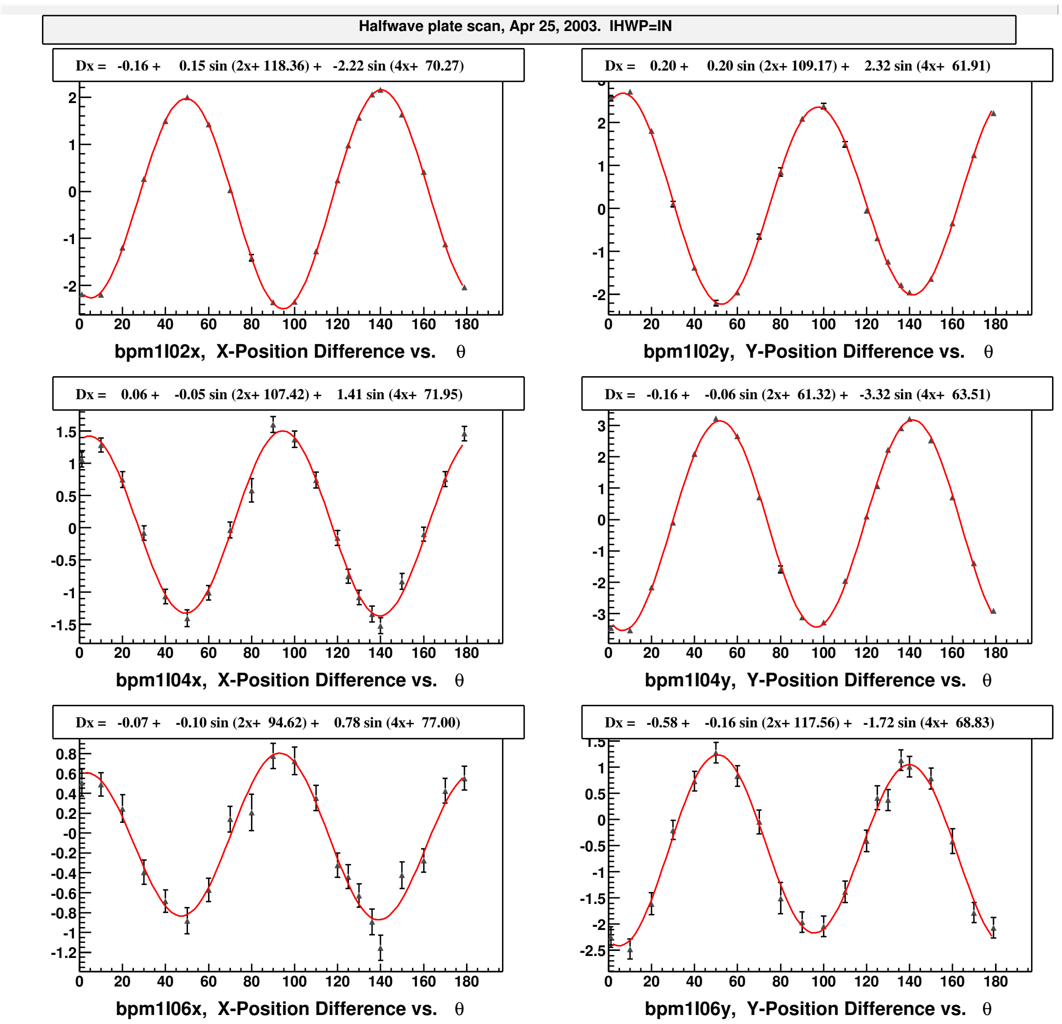

Figure 25: Position differences (in μm) measured by 100 keV BPMs during rotating waveplate scan. Insertable Halfwave Plate (IHWP) is IN. (PITA voltage P+= 7.224, P-= 7.457)

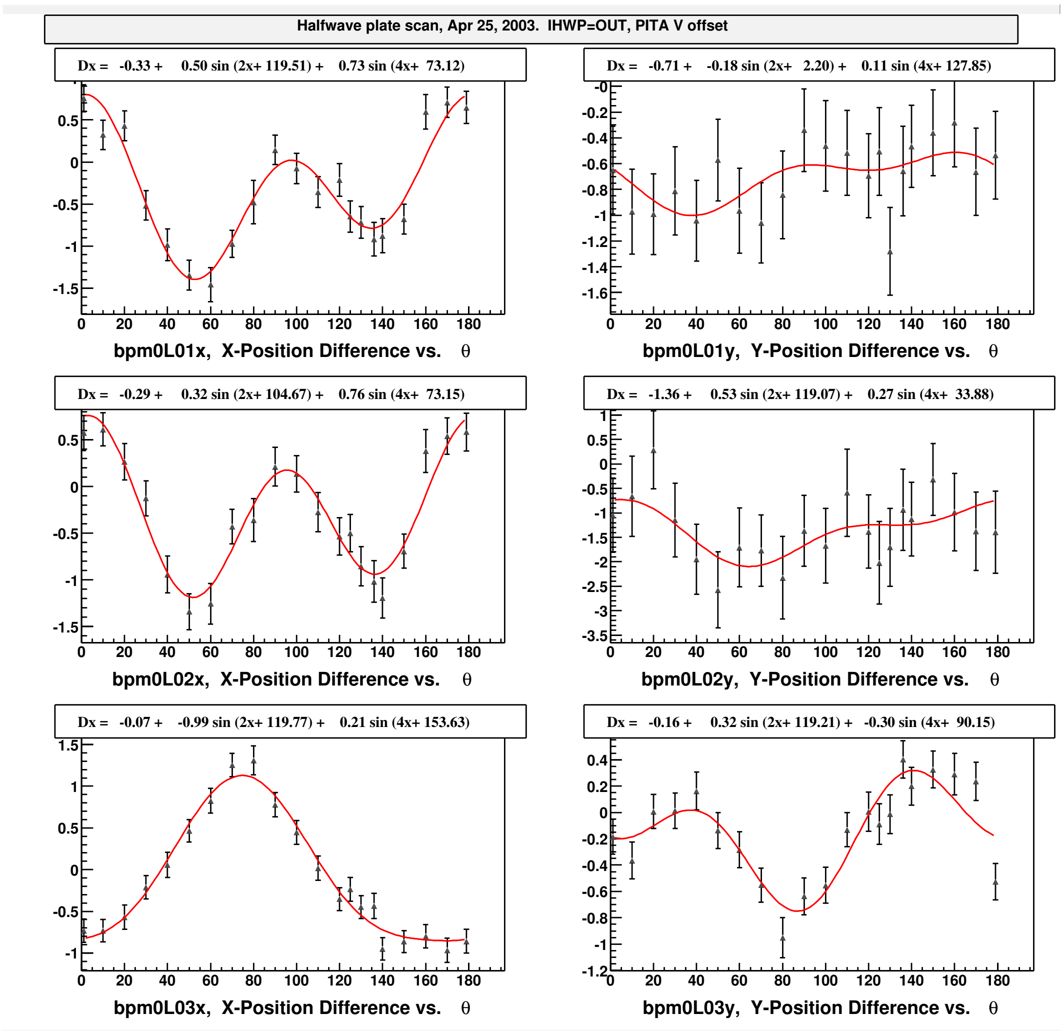

Figure 26: Position differences (in μm) measured in 5 MeV BPMs during rotating wave-plate scan. Insertable Halfwave Plate (IHWP) is OUT. PITA voltage is slightly offset (P+=7.154,P-=7.527).

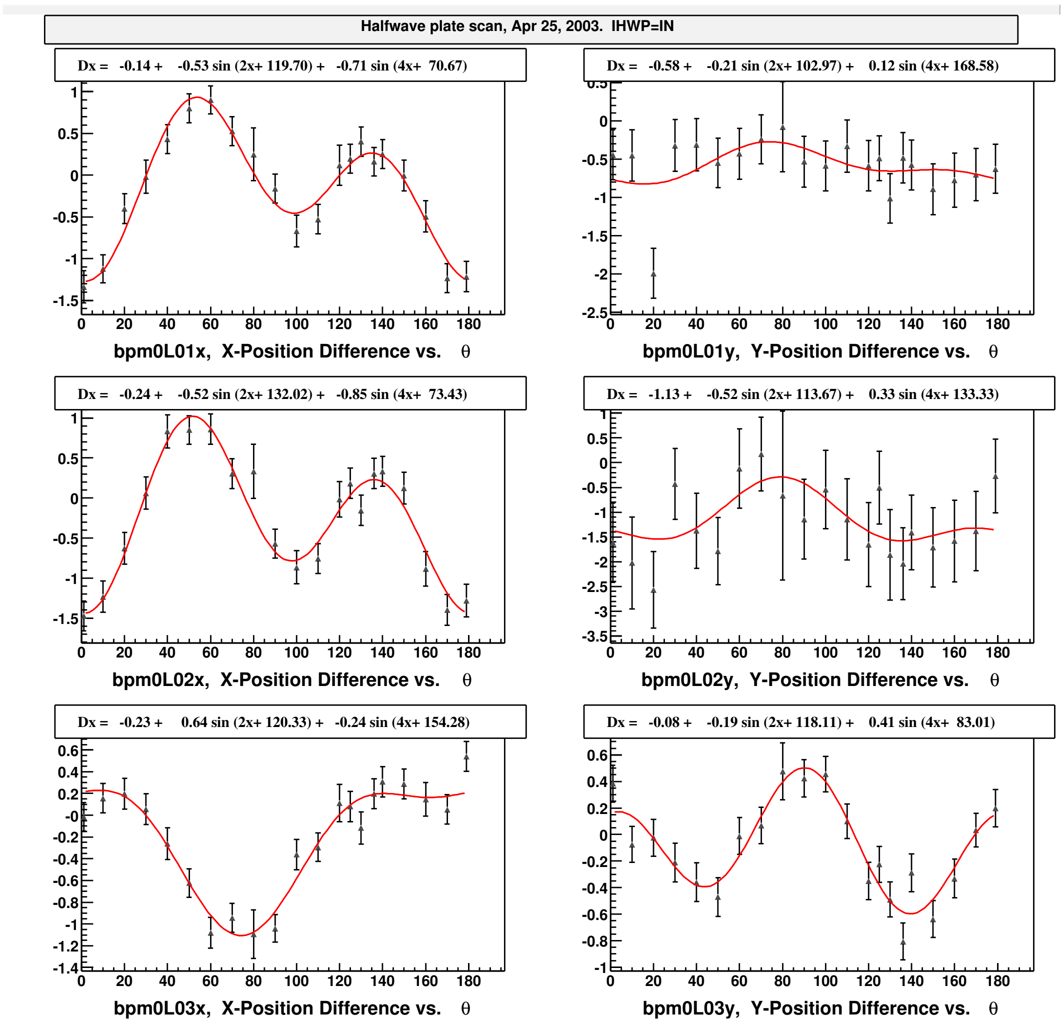

Figure 27: Position differences (in μm) measured in 5 MeV BPMs during rotating waveplate scan. Insertable Halfwave Plate (IHWP) is IN. (PITA voltage P+= 7.224, P-= 7.457)

5.3 Selected RHWP Setpoints

After consideration of the position differences, charge asymmetry, and charge asymmetry separation plots for both IHWP states, a RHWP setpoint for 30 degrees was chosen for both IHWP states.

The selected setpoint provided relatively small ($< 1\mu$m) position differences in 100 keV BPMs, with 8 ppm/Volt PITA slope and $<$ 500ppm charge asymmetry.

No advantage was seen to choosing different setpoints for each IHWP state, largely due to the dominance of the 4θ terms in position difference plots, with phases matching for both IHWP states and for both the x and y position differences. Only position difference plots from the 100 keV region were considered, in part to simplify the selection process.

6 RHWP Scans: Separation of Pair-Order Peaks

As discussed in Section 4.2, PZT mirror studies have shown helicity-correlated effects due to clipping on apertures in the injector. Injector clipping effects are evident in other studies of the beam tests, particularly in the charge asymmetry separation measured in the 5 MeV region (downstream of A1, A2, and the chopper).

Fig. 28 and Fig. 29 show the separation of charge asymmetry for symmetric and asymmetric pairs for RHWP scans with both IHWP states, measured at BCM 0L02 in the 5 MeV region. These plots are to be compared with measurements from the 100 keV region, shown in Fig. 14 and Fig. 15. The phase and amplitude of the θ-dependent terms are equivalent, but the 5 MeV results show a large offset for the asymmetric pair results. This result, which led to significant confusion during the tests, is now understood to arise from a helicity-correlated clipping of the asymmetric pairs arising from significant position differences (and *difference* in position differences) for the asymmetric pairs.

The separations in position difference for the symmetric and asymmetric pairs measured at BPMs in the 100 keV and 5 MeV regions during RHWP scans are shown in Figs. 30-33. The separations in the helicity-correlated position differences for the asymmetric pairs is large on the scale of HC systematics. It is particularly interesting to note that this separation does not scale with the position differences. Neglecting measurements from the 0L region (to avoid confusion due to aperture-clipping effects) the y position-difference separation $\Delta y_{\text{L-LR}} - \Delta y_{\text{R-RL}}$ is approximately 2μm, 3μm, -10μm in BPMs 1I02, 1I04 and 1I06, respectively, as seen in Fig. 30. For these BPMs, the size of the maximum Δy (averaged over all pair combinations) scales as -2.5μm, 4μm, and 1.5μm, as seen in Fig. 24.

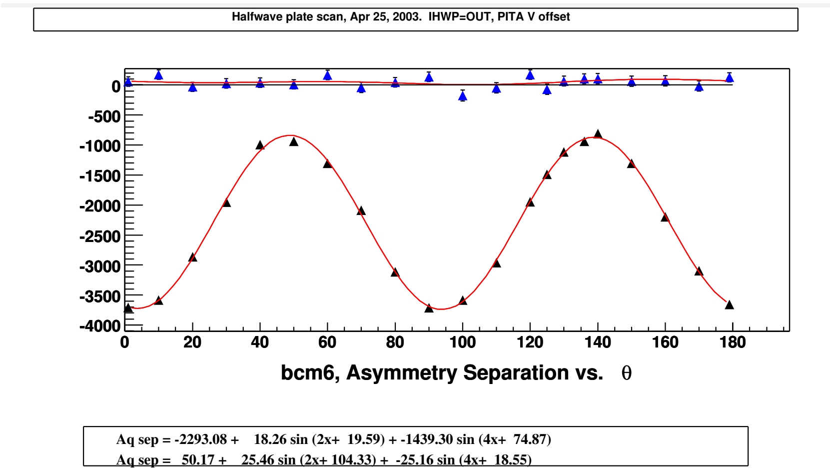

Figure 28: Separation between inner and outer peaks of charge asymmetry (in ppm) measured in BCM 0L02 during rotating waveplate scan. Insertable Halfwave Plate (IHWP) is OUT. PITA voltage is slightly offset (P+= 7.154,P-= 7.527).

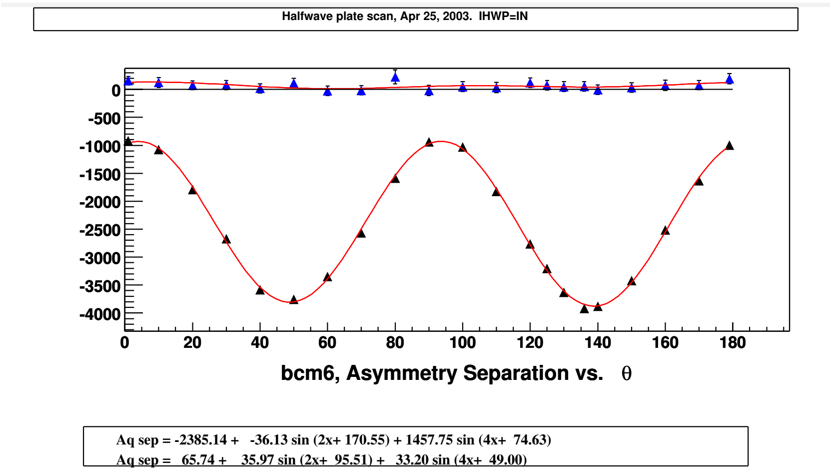

Figure 29: Separation between inner and outer peaks of charge asymmetry (in ppm) measured in BCM 0L02 during rotating waveplate scan. Insertable Halfwave Plate (IHWP) is IN. (PITA voltage P+= 7.224, P-= 7.457)

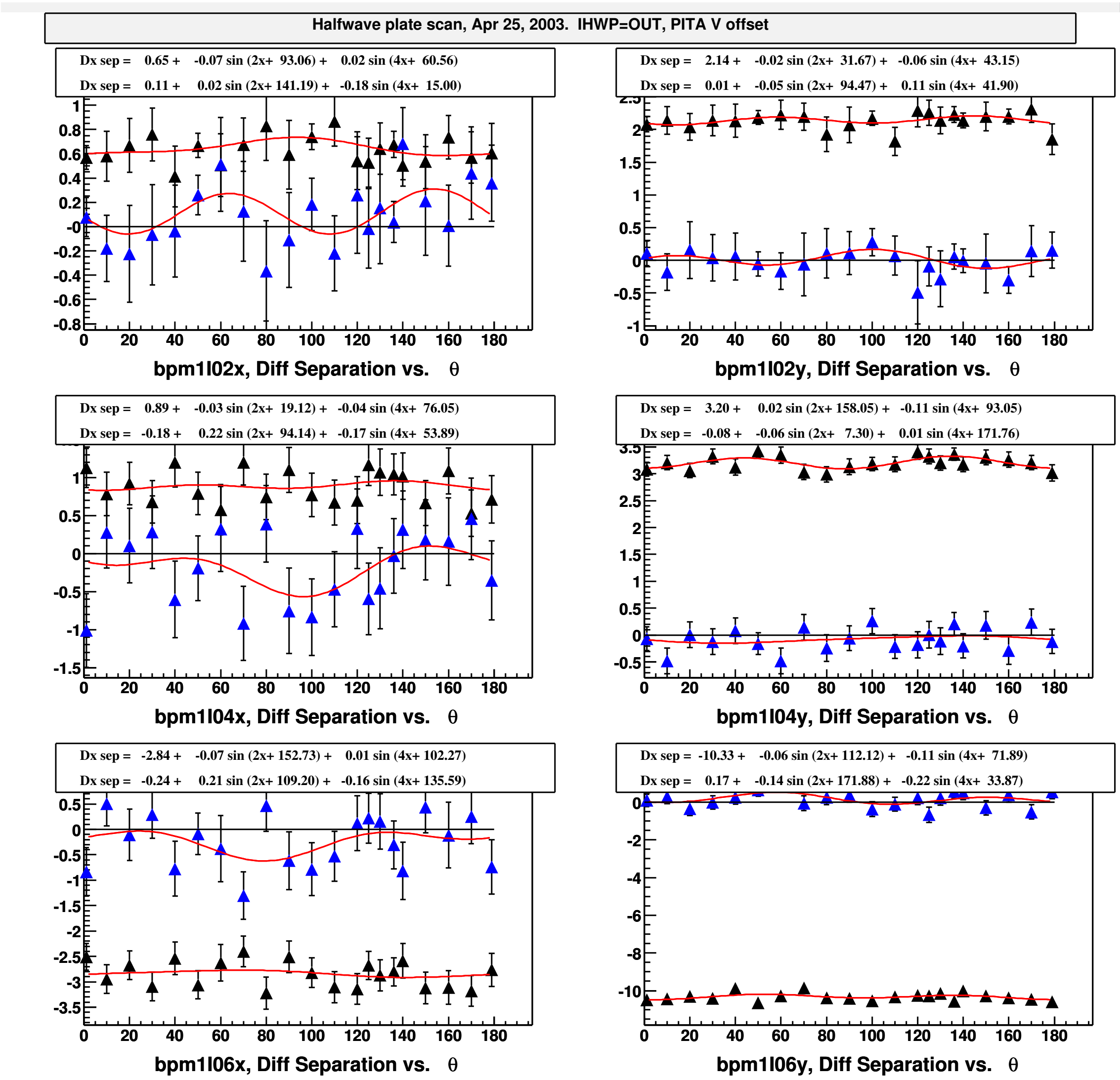

Figure 30: Separation of Position differences for outer and inner charge asymmetry peaks, measured by 100 keV BPMs during rotating waveplate scan. Insertable Halfwave Plate (IHWP) is OUT. PITA voltage is slightly offset (P+=7.154,P-=7.527).

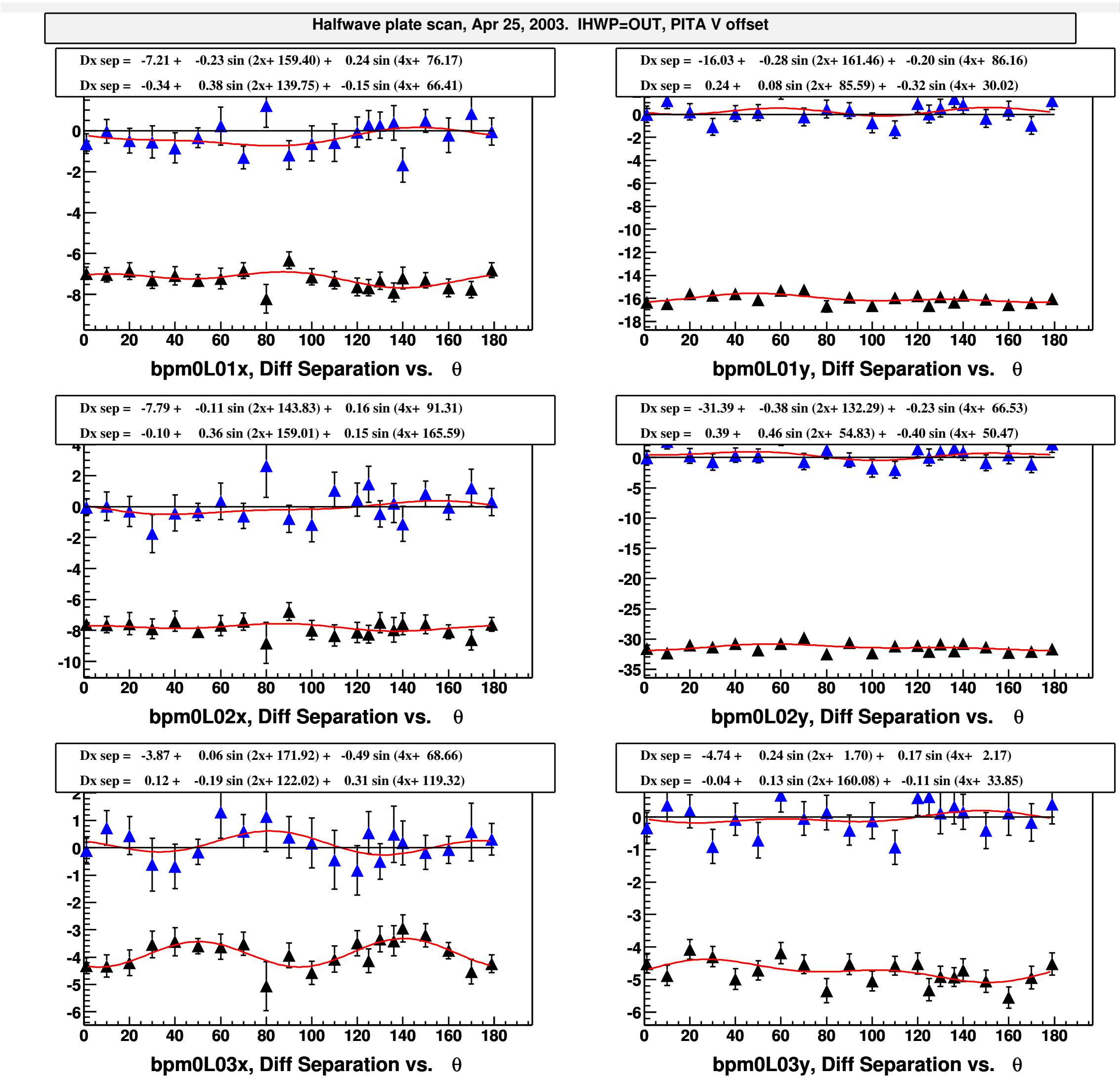

Figure 31: Separation of Position differences for outer and inner charge asymmetry peaks, measured in 5 MeV BPMs during rotating waveplate scan. Insertable Halfwave Plate (IHWP) is OUT. PITA voltage is slightly offset (P+=7.154,P-=7.527).

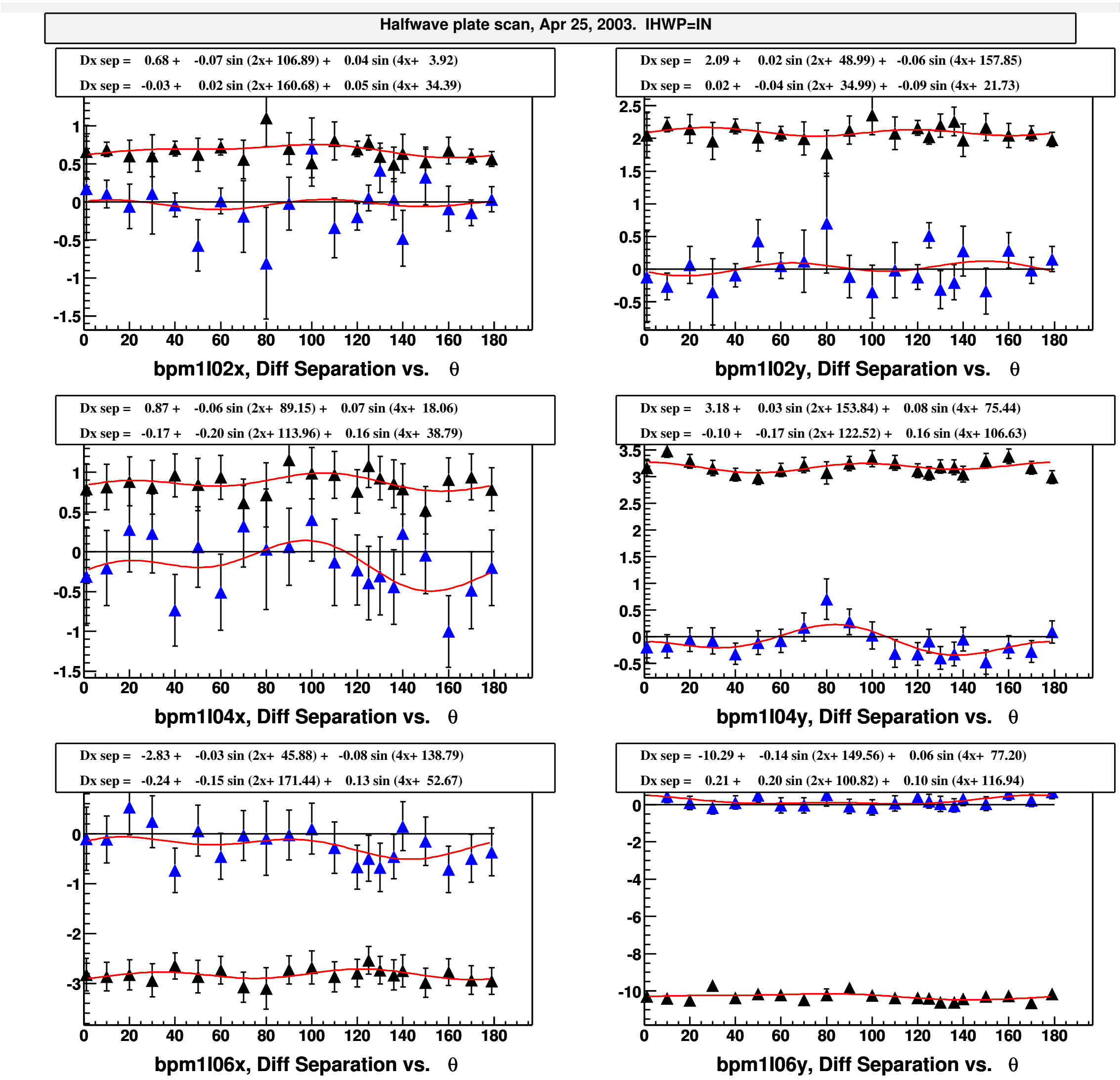

Figure 32: Separation of Position differences for outer and inner charge asymmetry peaks, measured by 100 keV BPMs during rotating waveplate scan. Insertable Halfwave Plate (IHWP) is IN. (PITA voltage P+= 7.224, P-= 7.457)

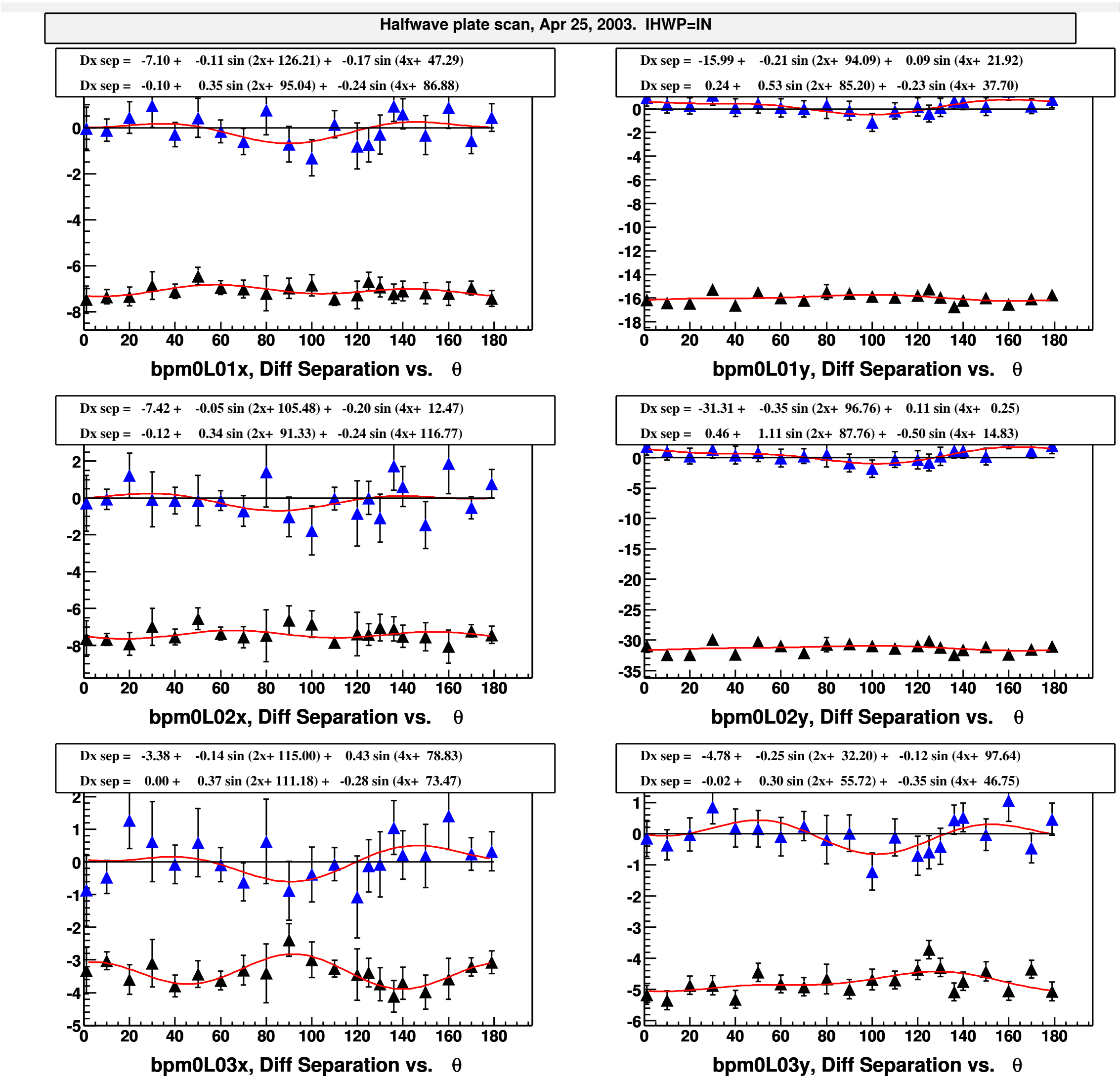

Figure 33: Separation of Position differences for outer and inner charge asymmetry peaks, measured in 5 MeV BPMs during rotating waveplate scan. Insertable Halfwave Plate (IHWP) is IN. (PITA voltage P+= 7.224, P-= 7.457)

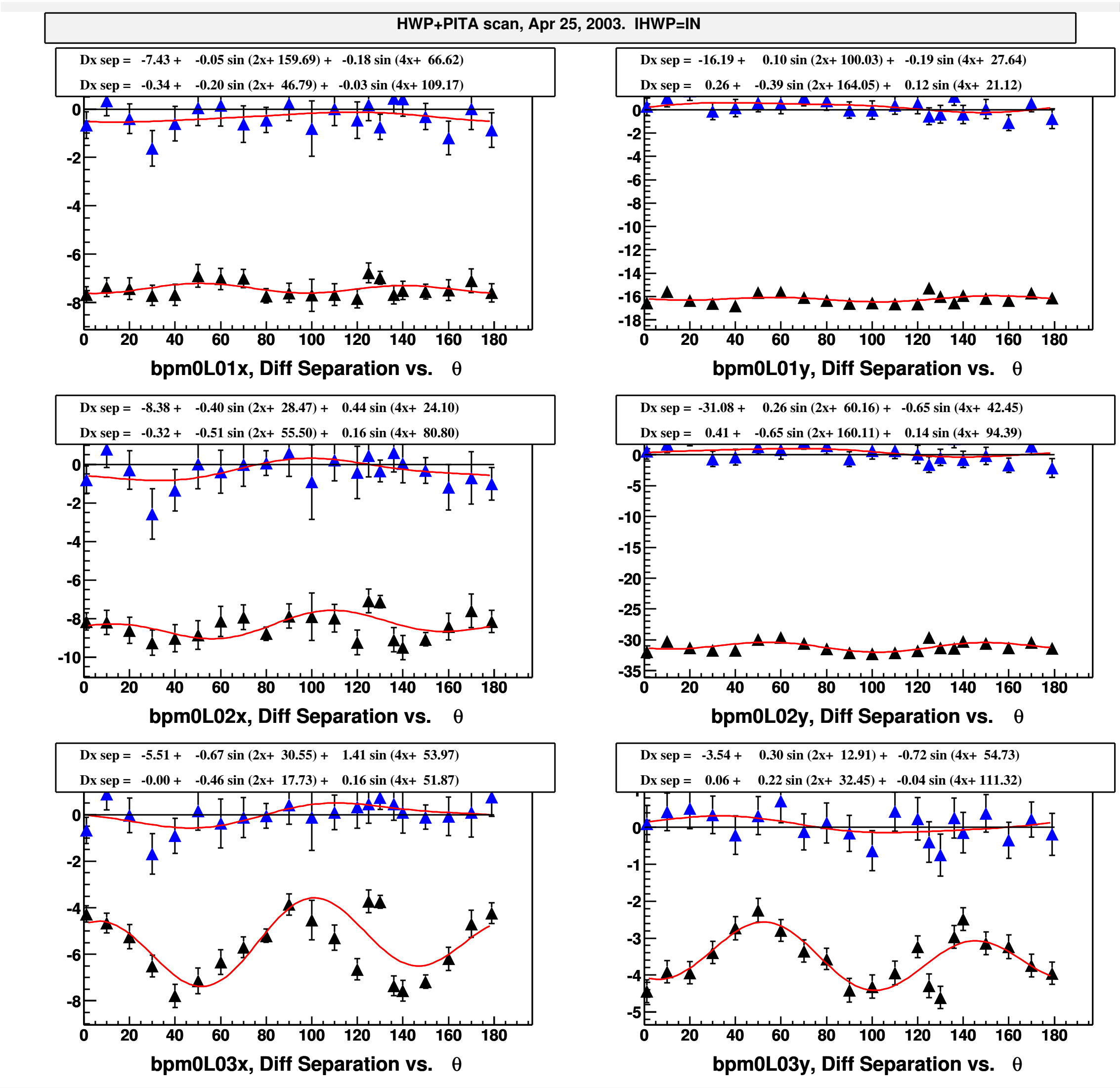

Figure 34: Separation of Position differences for outer and inner charge asymmetry peaks, measured in 5 MeV BPMs during rotating waveplate scan, with the PITA voltage at each waveplate setting used to zero charge asymmetry. Insertable Halfwave Plate (IHWP) is IN. Compare to 32.

7 Correlation of Position Differences with PITA Voltage

In order to verify the assumption that the outer peak separation is proportional to PITA slope, the PITA slope was measured at several RHWP angles.

Fig. 35 shows results for these PITA calibration curves. Figures 36-38 show the effect of the PITA voltage scan on position differences in the 100 keV region. At a small PITA slope, the position differences change by as much as .25 nm per ppm of A_Q change (for example, Δx measured in BPM 1I06, Fig. 38), while at large PITA slope magnitude this dependence is smaller by approximately a factor of 2.

As discussed in detail in Section 8, a gradient in the analyzing power of the photocathode would create a correlation between position differences and PITA voltage. Position differences resulting from residual linear polarization in the laser spot interacting with a cathode gradient should scale with PITA slope. As seen in Fig. 36 and Fig. 37, Δy measured in BPMs 1I02 and 1I04 appear to have this behavior, flipping sign with the PITA slope. However, as seen in Fig. 38, these sensitivities do not scale down proportionally with a reduced PITA slope magnitude. In addition, these plots show no apparent relationship between the PITA slope and Δx or ΔY measured in other BPMs. With these mixed results, it is not clear that a cathode gradient effect is indicated, and there has yet to emerge an alternative model to explain these results.

Figures 39-41 show similar measurements for the 5 MeV region, which may be effected by aperture clipping effects.

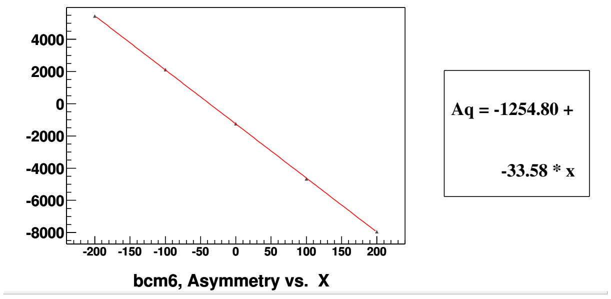

(a)

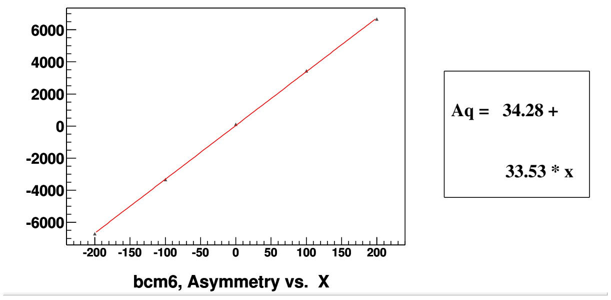

(b)

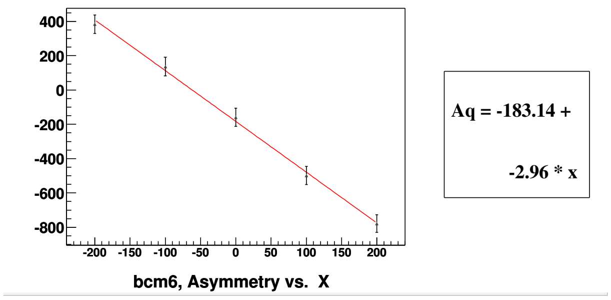

(c)

Figure 35: PITA slope calibrations expected to be minimum, maximum, and near zero, corresponding, in order, to RHWP = 95°, 140°, 115°. Insertable Halfwave Plate (IHWP) is IN.

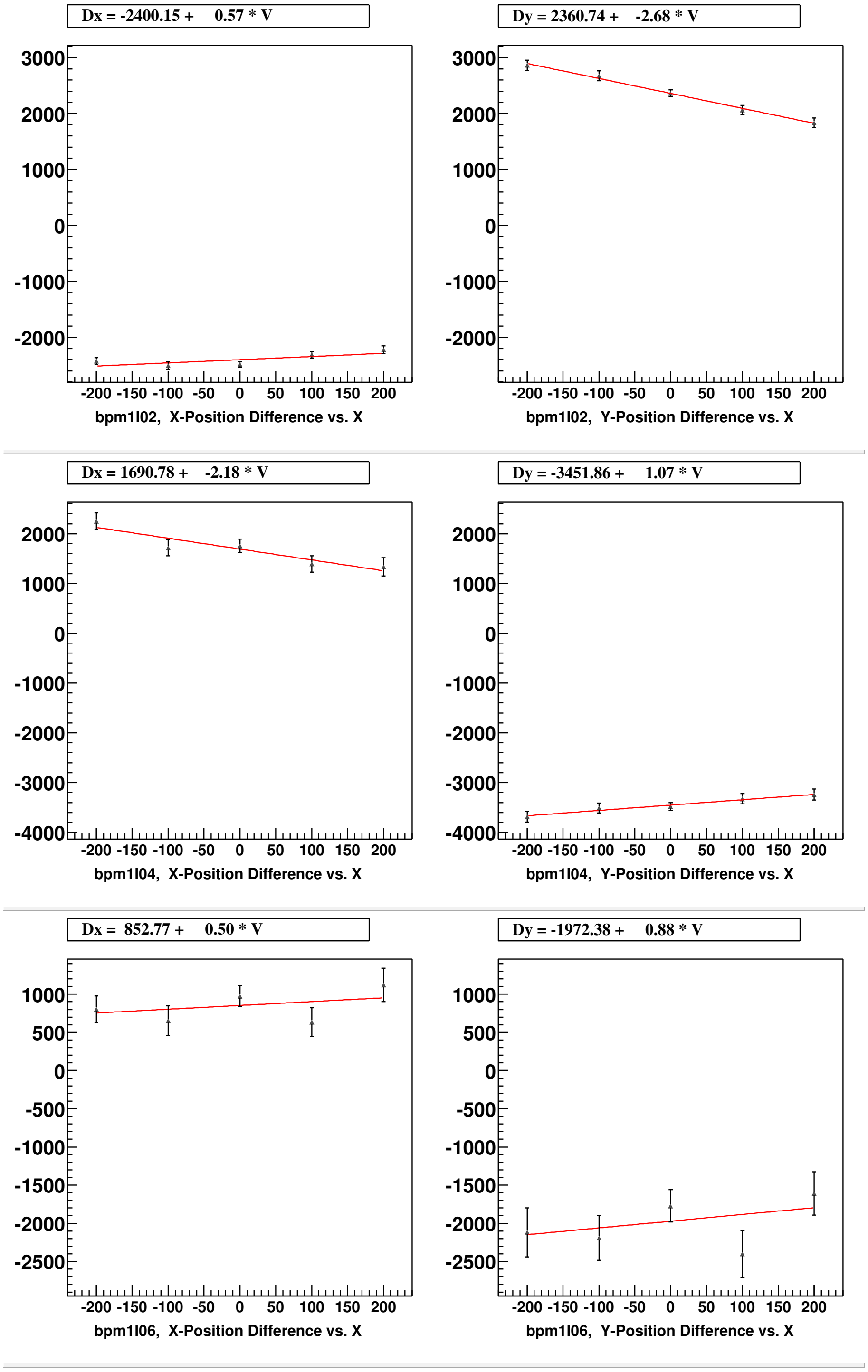

Figure 36: Position differences (in nm) in 100 keV region for PITA scan. RHWP = 95°, corresponding to a PITA slope of approximately −33ppm/Volt. Insertable Halfwave Plate (IHWP) is IN.

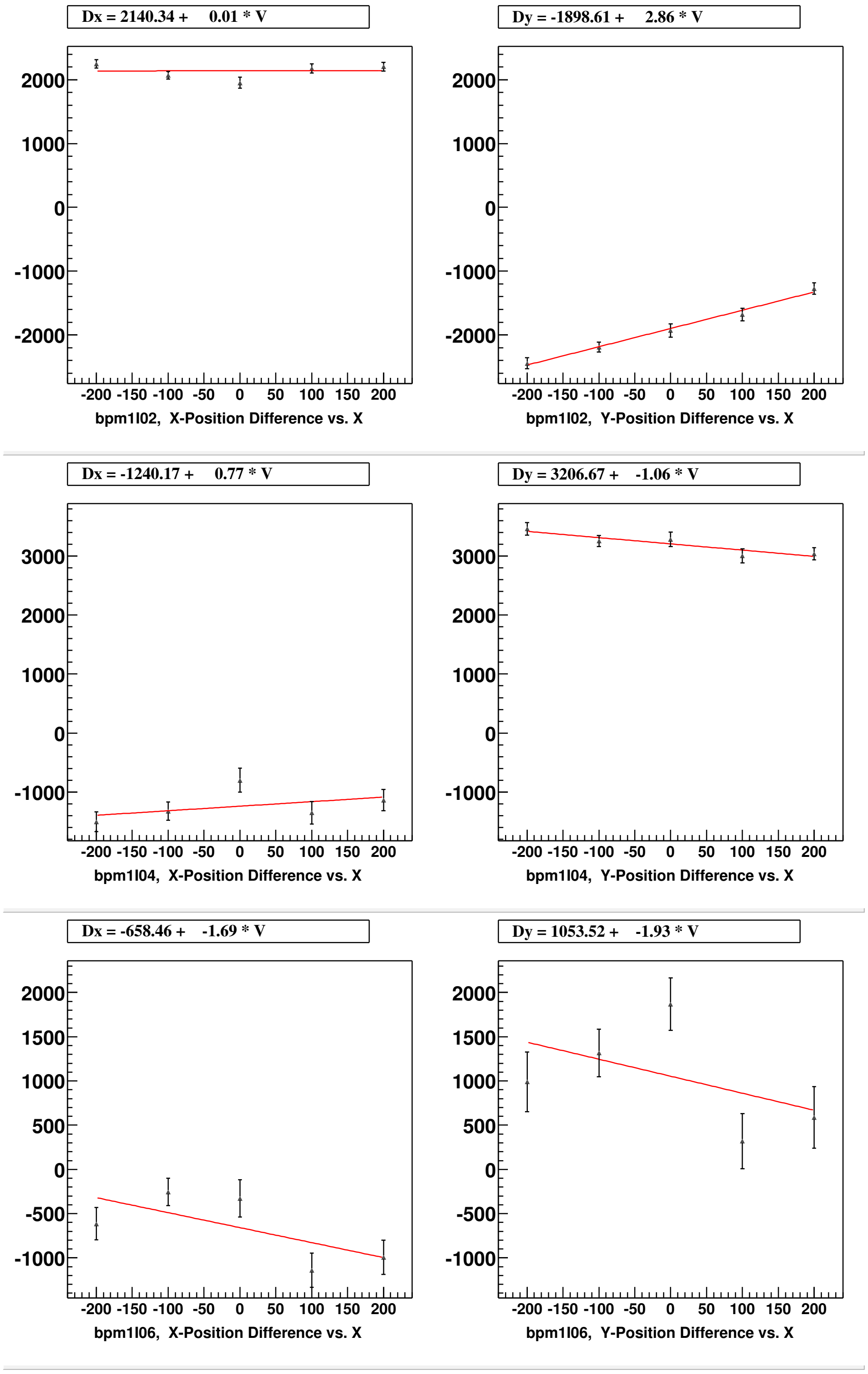

Figure 37: Position differences (in nm) in 100 keV region for PITA scan. RHWP = 140°, corresponding to a PITA slope of approximately 33ppm/Volt. Insertable Halfwave Plate (IHWP) is IN.

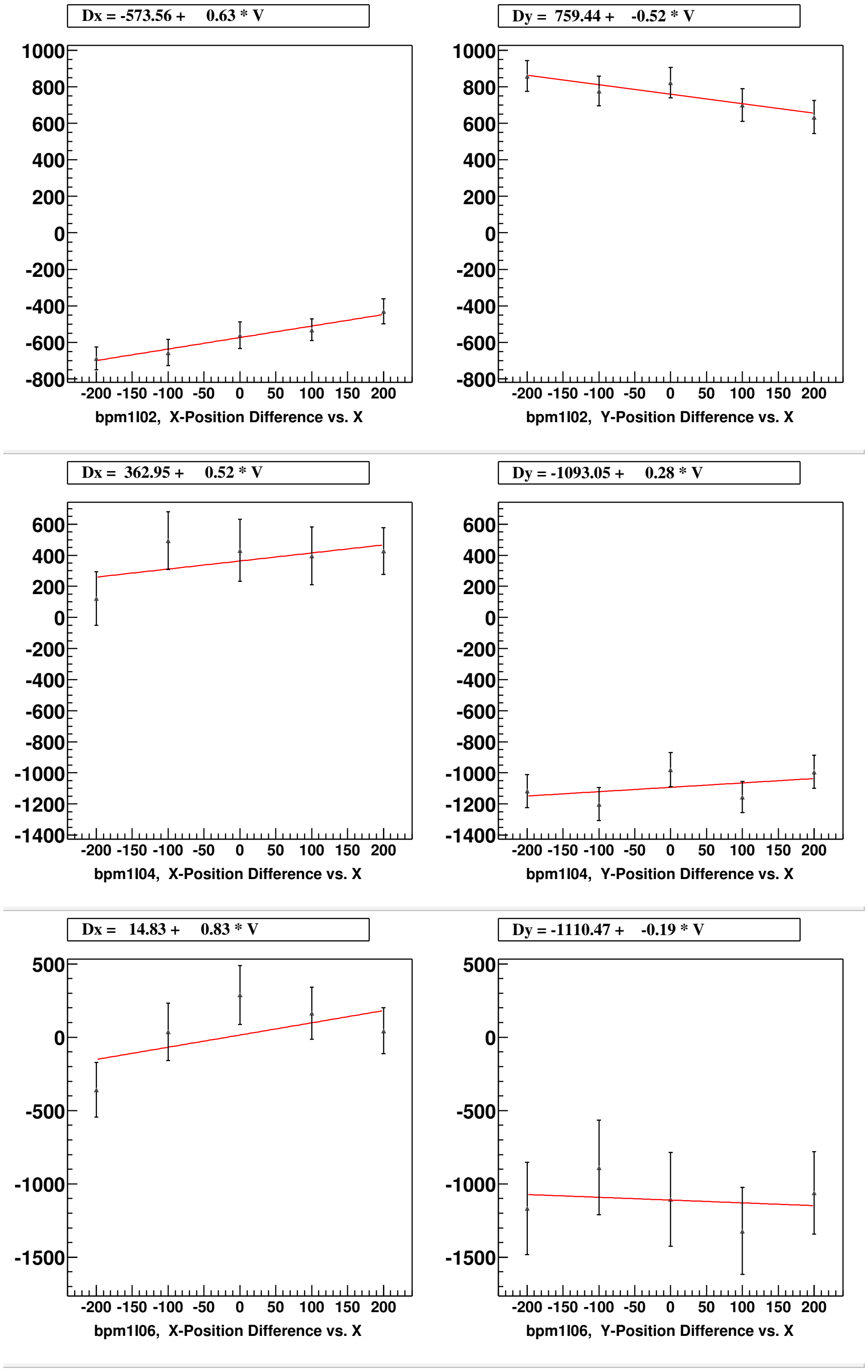

Figure 38: Position differences (in nm) in 100 keV region for PITA scan. RHWP = 115°, corresponding to a PITA slope of approximately −3ppm/Volt. Insertable Halfwave Plate (IHWP) is IN.

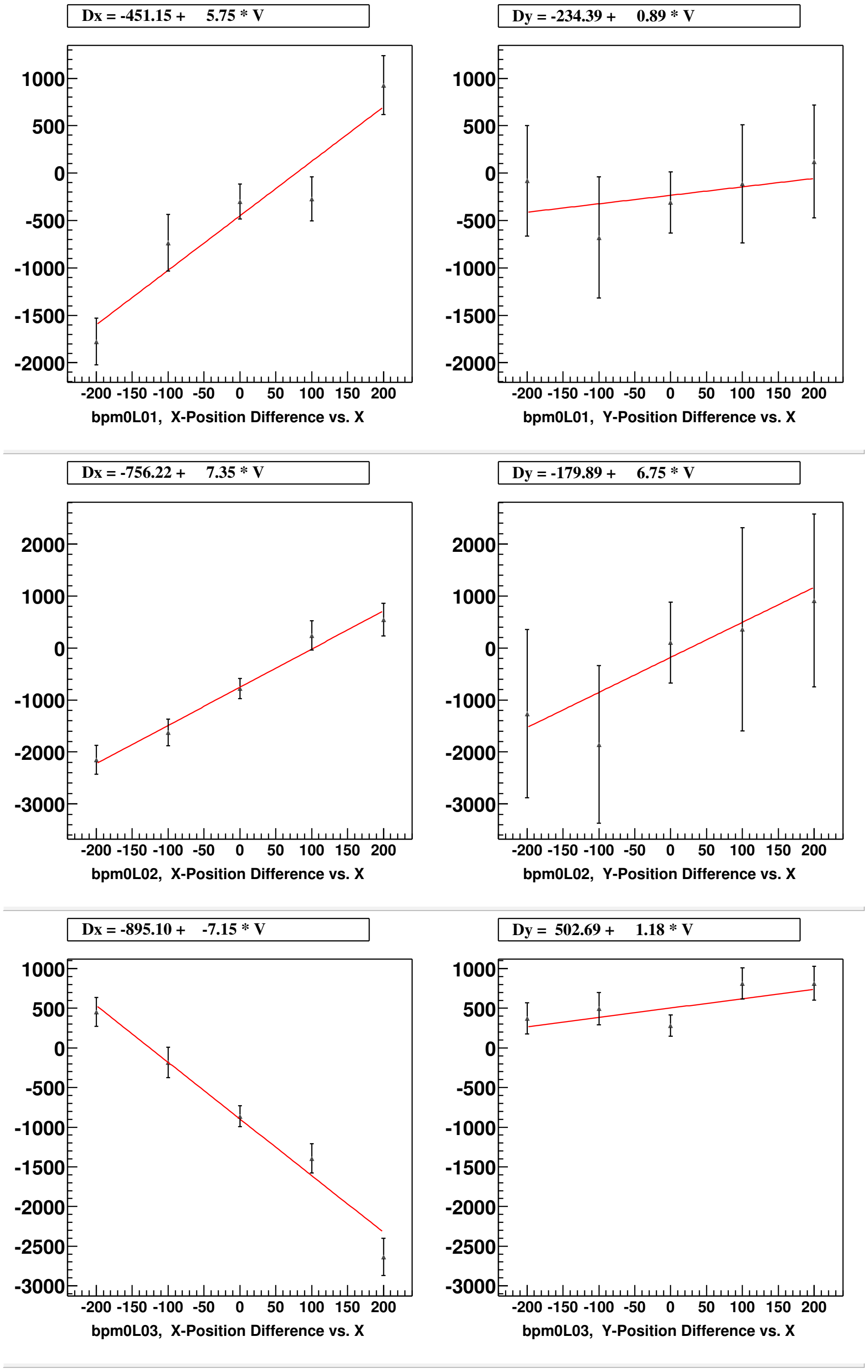

Figure 39: Position differences (in nm) in 5 MeV region for PITA scan. RHWP = 95°, corresponding to a PITA slope of approximately −33ppm/Volt. Insertable Halfwave Plate (IHWP) is IN.

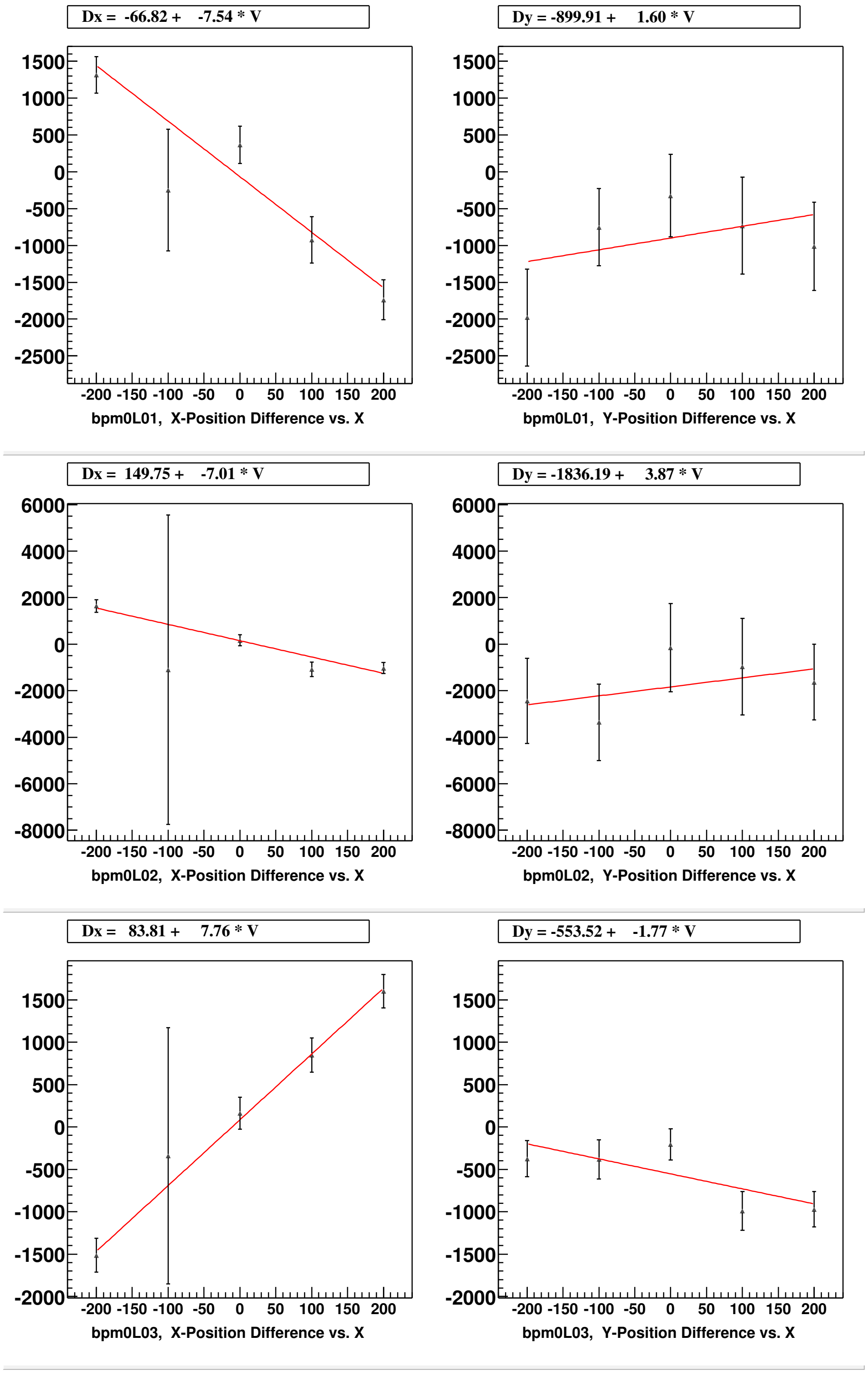

Figure 40: Position differences (in nm) in 5 MeV region for PITA scan. RHWP = 140°, corresponding to a PITA slope of approximately 33ppm/Volt. Insertable Halfwave Plate (IHWP) is IN.

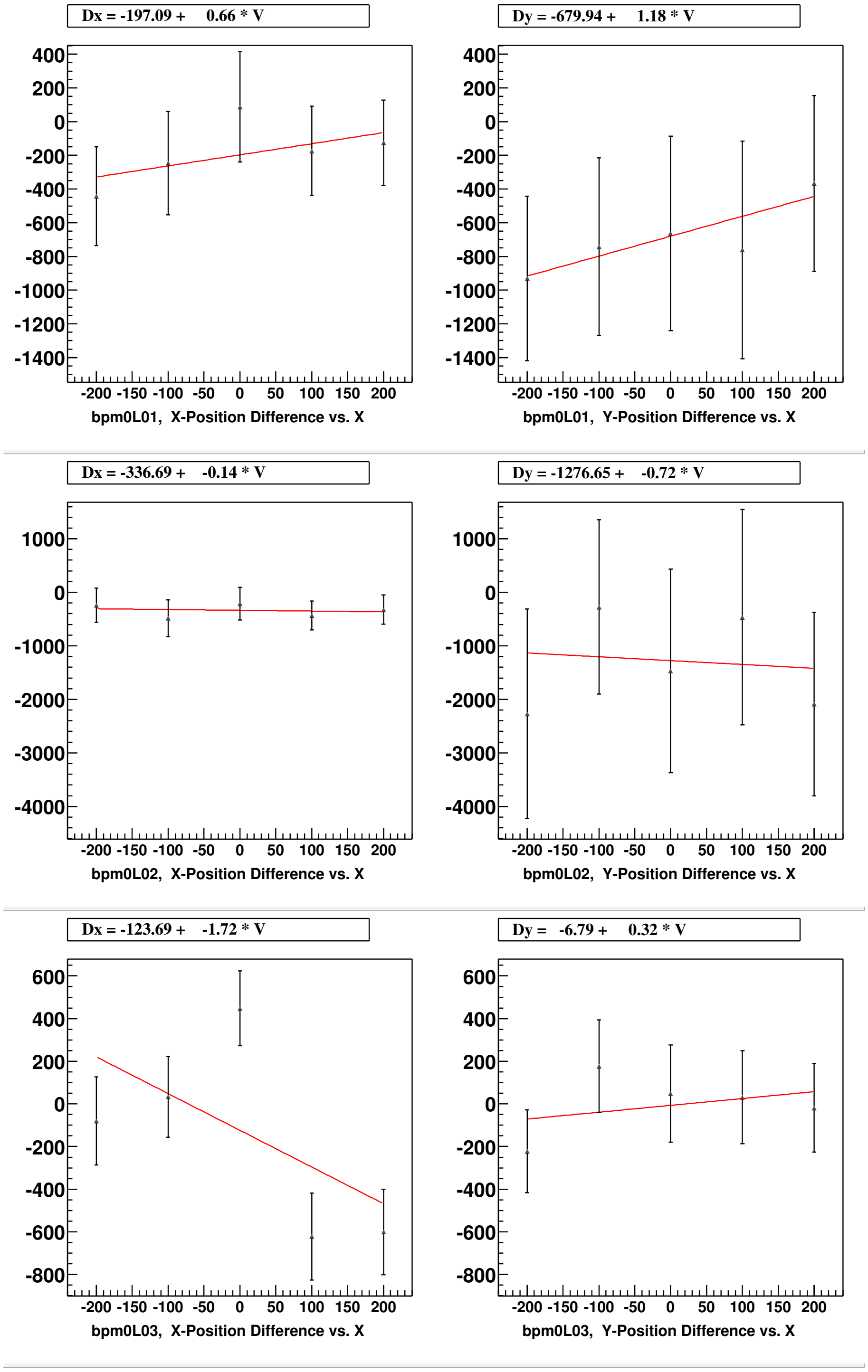

Figure 41: Position differences (in nm) in 5 MeV region for PITA scan. RHWP = 115°, corresponding to a PITA slope of approximately −3ppm/Volt. Insertable Halfwave Plate (IHWP) is IN.

8 Sources of Position Differences

There are four sources of position differences which are reasonably expected to be most significant for these measurements:

- **Steering/Lensing:** The Pockels cell may steer or lens the beam, thus creating helicity-correlated position differences. We have two models for how such an effect might arise, but do not know if either is correct. First, KD*P Pockels cells are piezo-electric, as well as electro-optic, so it is possible to have voltage-dependent physical deformation of the cell which would produce steering or lensing. Second, nonuniformities in the electric field could produce helicity-correlated gradients in the cell's indices of refraction that would turn the cell into a gradient-index lens.

- **Birefringence Gradient:** Each Pockel cell possesses a stress-induced birefringence (at zero applied voltage), which is not constant over the cross section of the cell. The gradient in this intrinsic birefringence persists when voltage is applied, leading to a relative phase retardation between orthogonal polarization states and thus a degree of linear polarization (DOLP) which is position dependent. The residual linear polarization, varying across the beam spot, interacts with the analyzing power of the photocathode and changes the average beam position by distorting the profile of the beam. The orientation of residual polarization is different for the two helicity states, so the beam-profile distortion produces a helicity-correlated average position difference.

- **Cathode Gradients:** The analyzing power of the strained GaAs photocathode could vary significantly over the beam spot. Such a variation would interact with the residual linear polarization in the laser (even if this residual polarization is constant over the beam spot) to distort the intensity profile of the beam. Similar to the birefringence gradient, this produces a helicity-correlated average position difference.

- **Vacuum Window Birefringence Gradients:** A birefringence gradient in the vacuum window (which presumably acquires some stress-induced birefringence from the strain of its mounting and the pressure difference across it) can act in the same way as Pockels cell birefringence gradients, creating a position-dependent DOLP which leads to a helicity-correlated distortion of the beam intensity profile.

The RHWP scans and PITA voltage setpoints are useful tools for distinguishing between these mechanisms. Steering/Lensing effects do not depend on the degree of circular polarization or the orientation of residual linear polarization, so they will remain constant while rotating the halfwave plate. A vacuum-window birefringence gradient will also be insensitive to the RHWP setpoint, as it does not depend on the orientation of residual linear polarization from the Pockels cell. Both Pockels-cell birefringence gradients and cathode analyzing-power gradients are sensitive to the relative orientation of linear polarization in the laser and analyzing power on the cathode. Therefore, they scale as $\sin 4\theta$ for a RHWP scan. Performing an RHWP scan provides a quick indication of the relative strengths of the steering (constant term) and the gradient effects (4θ term).[1]

The IHWP provides an easy check on this determination. By inverting the Left and Right circular polarization states relative to Pockels cell voltage, the IHWP rotates the

[1]Additional terms can complicate this picture, but these effects can be neglected for the present discussion. A gradient in the RHWP itself creates a term proportional to 2θ, and the effect of a gradient in the vacuum window is constant for an RHWP scan.

orientation of residual linear polarization from all downstream elements by 90°. This change in direction of linear polarization will flip the sign of effects from cathode gradients and birefringence gradients in the Pockels cell and vacuum window. Steering effects do not depend on polarization, and so are unaffected.

It is further possible to distinguish between birefringence gradients and cathode gradients using the PITA voltage offset. The degree of linear polarization is proportional to the PITA voltage offset. Cathode gradient effects are proportional to the average residual DOLP, while birefringence-gradient effects are only sensitive to the variation in the DOLP across the beam spot. A coupling between PITA voltage and Δx would imply a cathode gradient effect; a component of Δx independent of PITA voltage would imply either steering or birefringence effects.

Using these principles, the following conclusions are suggested from the results of these studies:

- The fit of position differences as a function of RHWP angle (for example, Fig. 24) reveals a negligible constant term, which implies that steering/lensing effects from the Pockels cell and birefringence gradients in the vacuum window are negligible relative to Pockels-cell gradient effects. The relative importance of steering or vacuum window effects is difficult to discern from comparison of these small terms between IHWP states (Figs. 24 and 25).

- Changing the PITA offset during an RHWP scan to zero charge asymmetry does not significantly change the parameters of the "$4\theta, 2\theta$" fit (for example, compare Fig. 20 and Fig. 24). This suggests that the dominant 4θ component of position differences arises primarily from birefringence gradients in the Pockels cell, rather than a cathode gradient. However, these scans do deviate in the range of RHWP from 40°-80° when the PITA offset voltages were significant, suggesting that the cathode gradient effect may not be entirely negligible.

- The dependence of position differences on PITA voltage does not entirely match the expected behavior for a cathode gradient effect. Nevertheless, the fact that such a dependence exists may hint at a cathode gradient effect or some other (previously unconsidered) mechanism for producing position differences from an asymmetric phase shift.

- The separation of position differences for asymmetric pairs shows very little response to RHWP angle (for example, Fig. 30). This suggests that the time-history effects are dominated by Pockels-cell steering effects. This conclusion is somewhat surprising given that steering effects do not appear to create a significant net position difference.

9 Comparison to February Studies

A similar (though less ambitious) test program was performed in February, 2003. A different Pockels cell ("Merry") was in use at that time, and there were other minor differences in the source configuration. Comparison between results from February and April tests is useful for demonstrating how these effects might vary with individual Pockels-cell characteristics or injector parameters.

- Charge asymmetry separation (comparing Figures 14, 28, and 44) indicates an absence of significant clipping in the injector during the February tests. This separation behaves as expected, flipping sign with IHWP reversal (Fig. 45).
- Position differences (Fig. 46 and Fig. 47) display comparable effects from steering and birefringence or cathode gradients. This is in contrast with the April results, for which steering was a negligible contribution to position differences.
- The position difference separation for asymmetric pairs, shown in Fig. 48 and Fig. 49, displays a significant contributions from both birefringence or cathode gradients (4θ dependence) and steering effects (constant term).

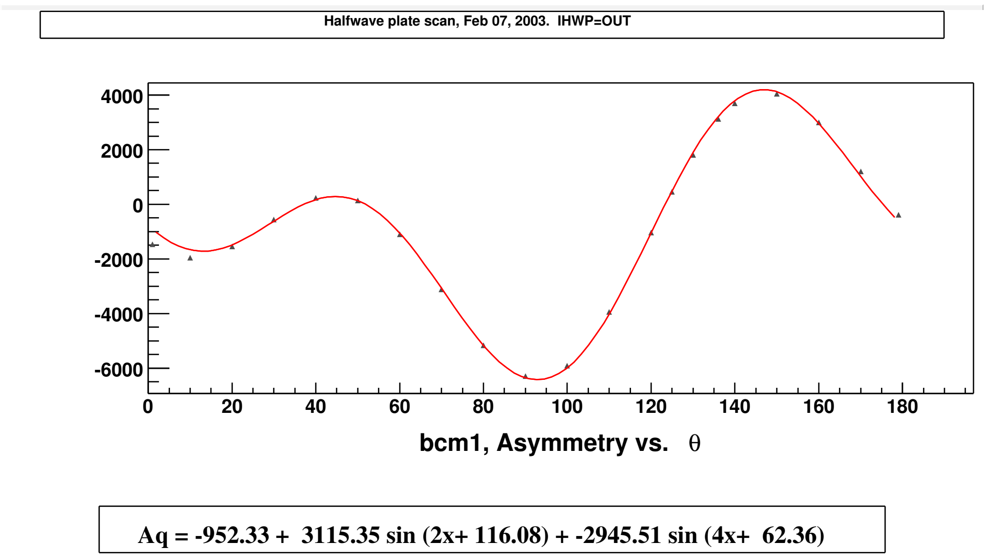

Figure 42: Charge asymmetry (in ppm) measured at BCM 0L02 for RHWP scan taken February 07, 2003. Insertable Halfwave Plate (IHWP) is OUT. Compare to Fig. 12.

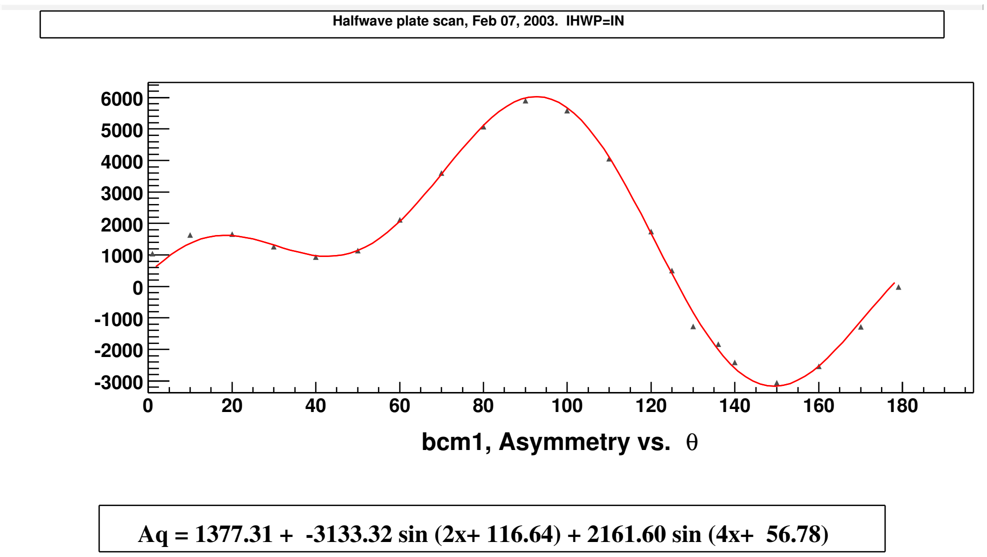

Figure 43: Charge asymmetry (in ppm) measured at BCM 0L02 for RHWP scan taken February 07, 2003. Insertable Halfwave Plate (IHWP) is IN. Compare to Fig. 13.

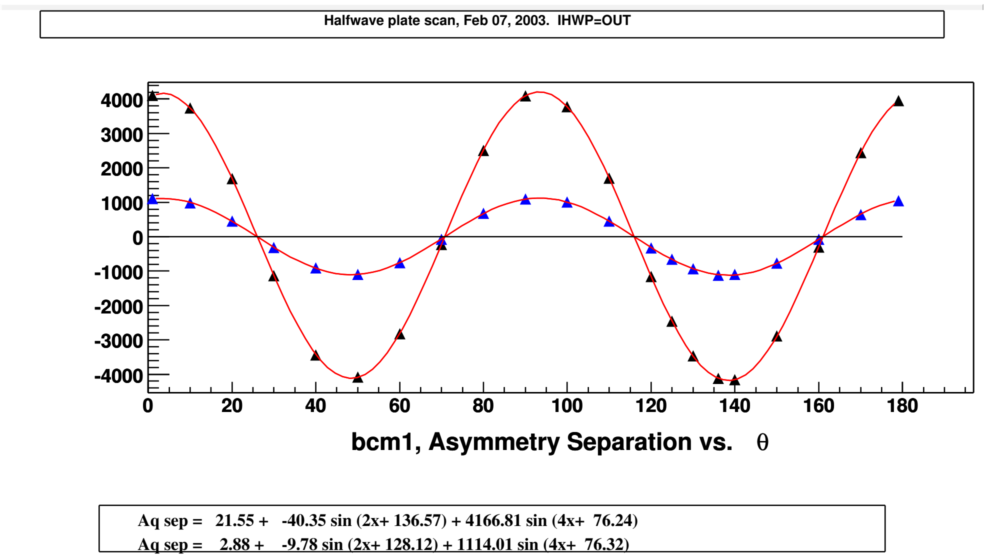

Figure 44: Charge asymmetry separation (in ppm) between symmetric and asymmetric pair combinations, measured at BCM 0L02 for RHWP scan taken February 07, 2003. Insertable Halfwave Plate (IHWP) is OUT. Compare to Fig. 14.

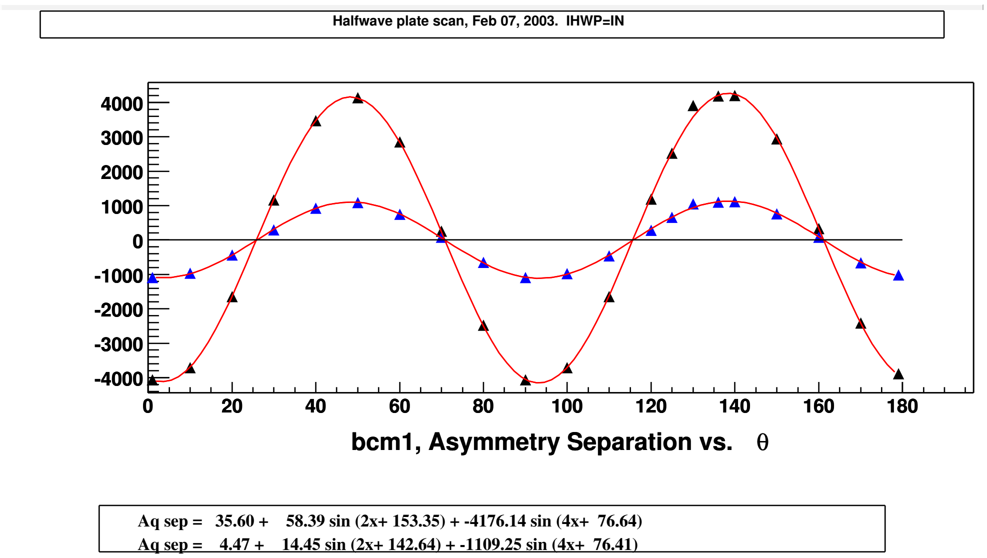

Figure 45: Charge asymmetry separation (in ppm) between symmetric and asymmetric pair combinations, measured at BCM 0L02 for RHWP scan taken February 07, 2003. Insertable Halfwave Plate (IHWP) is IN. Compare to Fig. 15.

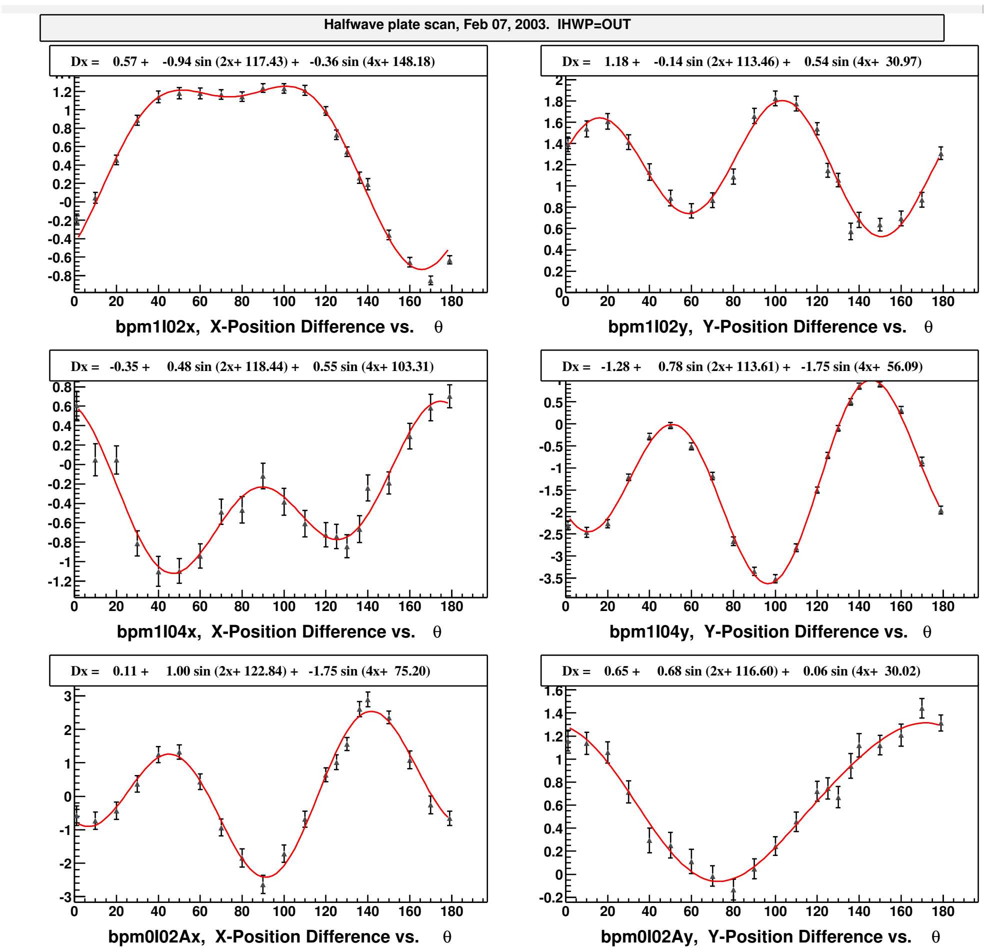

Figure 46: Position Differences (in μm) at various 100 keV BPMs for RHWP scan taken February 07, 2003. Insertable Halfwave Plate (IHWP) is OUT. Two BPMs are the same as those measured in April, compare with Fig. 24.

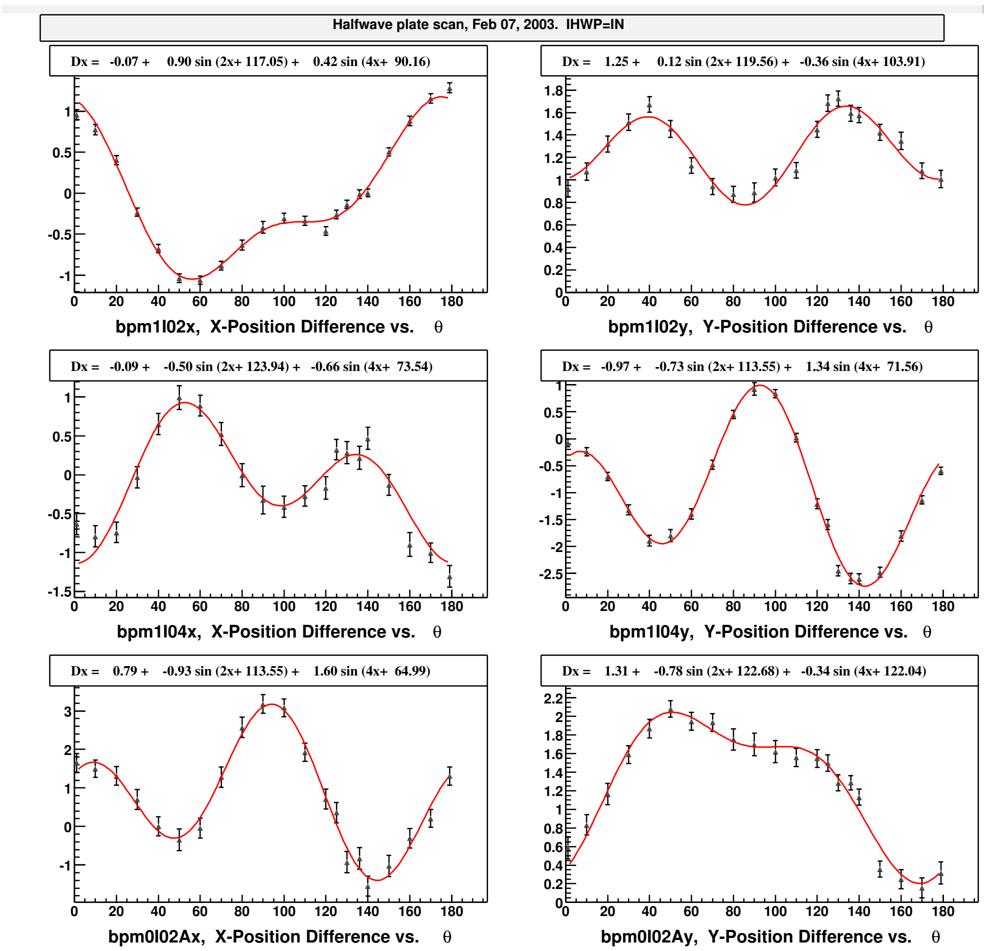

Figure 47: Position Differences (in μm) at various 100 keV BPMs for RHWP scan taken February 07, 2003. Insertable Halfwave Plate (IHWP) is IN. Two BPMs are the same as those measured in April, compare with Fig. 25.

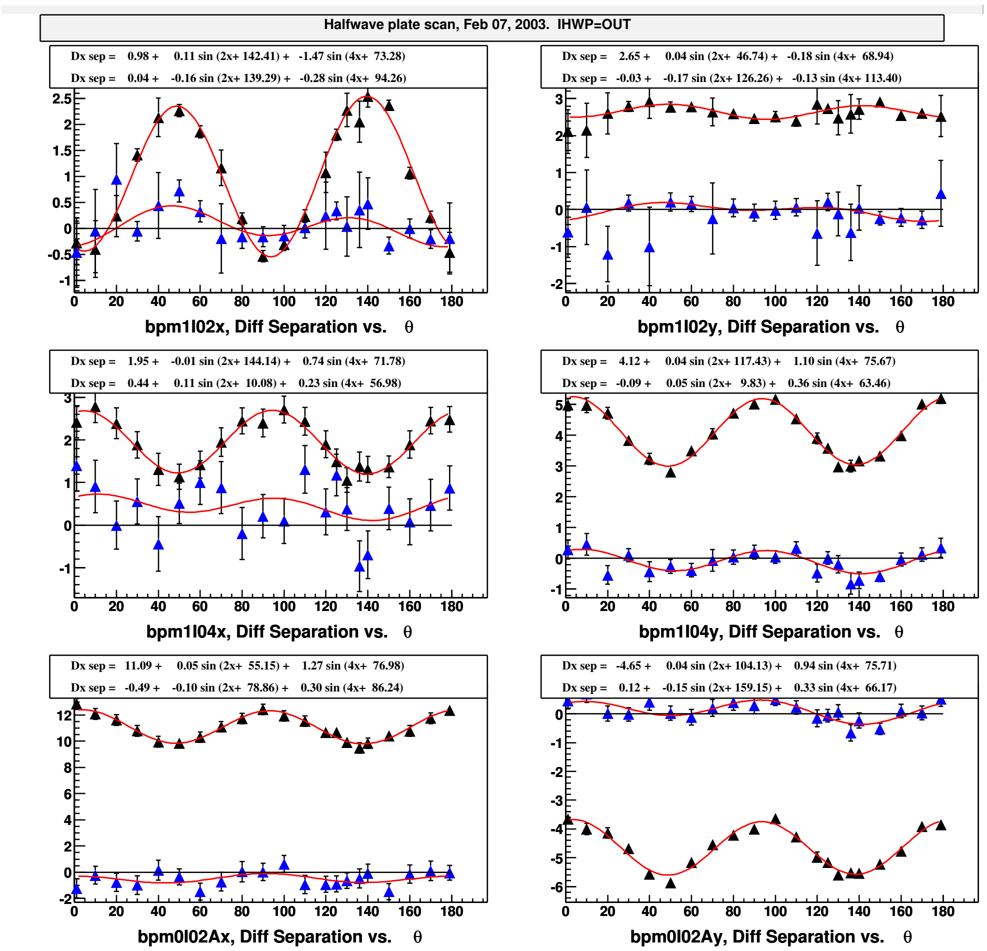

Figure 48: Separation in Position Difference (in μm) between symmetric and asymmetric pair combinations, measured at various 100 keV BPMs for RHWP scan taken February 07, 2003. Insertable Halfwave Plate (IHWP) is OUT. Two BPMs are the same as those measured in April, compare with Fig. 30.

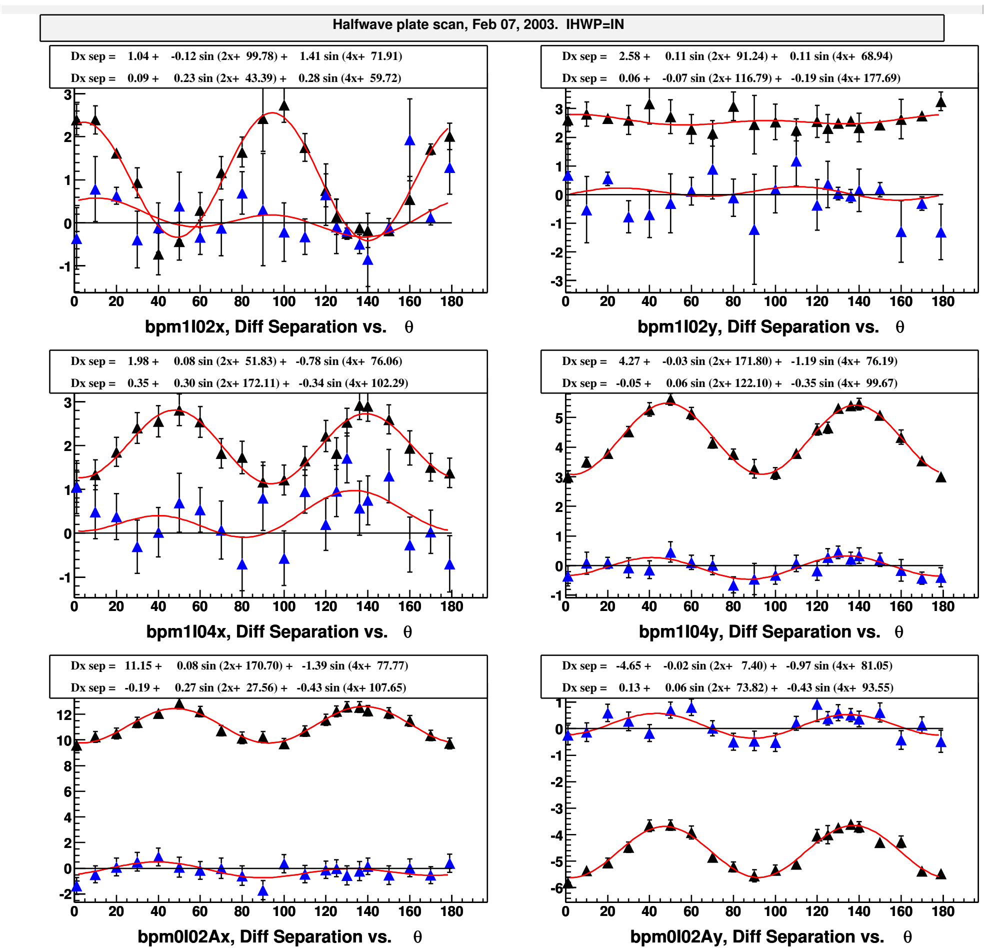

Figure 49: Separation in Position Difference (in μm) between symmetric and asymmetric pair combinations, measured at various 100 keV BPMs for RHWP scan taken February 07, 2003. Insertable Halfwave Plate (IHWP) is IN. Two BPMs are the same as those measured in April, compare with Fig. 32.